NASA.14:D-8433

OCT 5 1977

NASA TECHNICAL NOTE

NASA TN D-8433

COMPLETED
ORIGINAL

NASA TN D-8433

EXPERIMENTAL DESIGN STUDIES AND FLOW VISUALIZATION OF PROPORTIONAL LAMINAR-FLOW FLUIDIC AMPLIFIERS

R. F. Hellbaum and J. N. McDermon

Langley Research Center
Hampton, Va. 23665

NATIONAL AERONAUTICS AND SPACE ADMINISTRATION • WASHINGTON D. C. • AUGUST 1977

42

1 Report No.	2 Government Accession No.	3 Recipient's Catalog No.
NASA TN D-8433		

4 Title and Subtitle	5 Report Date
EXPERIMENTAL DESIGN STUDIES AND FLOW VISUALIZATION OF PROPORTIONAL LAMINAR-FLOW FLUIDIC AMPLIFIERS	August 1977
	6 Performing Organization Code

7 Author(s)	8 Performing Organization Report No.
R. F. Hellbaum and J. N. McDermon	L-10868
	10 Work Unit No.
	512-52-02-01
9 Performing Organization Name and Address	11 Contract or Grant No.
NASA Langley Research Center Hampton, VA 23665	
	13 Type of Report and Period Covered
12 Sponsoring Agency Name and Address	Technical Note
National Aeronautics and Space Administration Washington, DC 20546	14 Sponsoring Agency Code

15 Supplementary Notes

Technical Film Supplement L-1228 available on request.

16 Abstract

An experimental program was initiated at the Langley Research Center to study the effects of certain parameter variations on the performance characteristics of laminar, proportional, jet-deflection fluidic amplifiers. The matching and staging of amplifiers to obtain high pressure gain was included, but dynamic effects were not. The parameter variations considered were aspect ratio, setback, control length, splitter distance, receiver-duct width, width of center-vent duct, and bias pressure. Usable pressure gains of 19 per stage were achieved, and 5 amplifier stages were integrated to yield an overall pressure gain of 2 000 000.

17 Key Words (Suggested by Author(s))	18 Distribution Statement
Fluidics (fluidic amplifiers) Laminar flow Flow visualization	Unclassified - Unlimited Subject Category 34

19 Security Classif. (of this report)	20 Security Classif. (of this page)	21 No. of Pages	22 Price*
Unclassified	Unclassified	38	$4.00

* For sale by the National Technical Information Service, Springfield, Virginia 22161

EXPERIMENTAL DESIGN STUDIES AND FLOW VISUALIZATION OF PROPORTIONAL LAMINAR-FLOW FLUIDIC AMPLIFIERS

R. F. Hellbaum and J. N. McDermon
Langley Research Center

SUMMARY

An experimental program was initiated at the Langley Research Center to study the effects of certain parameter variations on the performance characteristics of laminar, proportional, jet-deflection fluidic amplifiers. The matching and staging of amplifiers to obtain high pressure gain was included, but dynamic effects were not. The parameter variations considered were aspect ratio, setback, control length, splitter distance, receiver-duct width, width of center-vent duct, and bias pressure. Usable pressure gains of 19 per stage were achieved, and 5 amplifier stages were integrated to yield an overall pressure gain of 2 000 000.

INTRODUCTION

Fluidic devices utilize flow phenomena to manipulate fluid signal intelligence which is represented by the fluidic quantities of pressure and flow. The application of fluidic devices for signal information control and amplification received great emphasis as a field of research in the 1960's. Early models of fluidic amplifiers usually operated in turbulent flow and had high noise levels and limited gain. Background information on the prior development and design of jet-deflection proportional amplifiers is described in reference 1, which includes a comprehensive source bibliography.

The purpose of the present investigation is to build and test laminar-flow jet-deflection proportional amplifiers in order to determine the effects of design-parameter variations on performance and to establish techniques of cascading amplifier stages for high overall gain. High-gain proportional fluidic amplifiers that are capable of sufficiently increasing the low-pressure signal levels, such as the output of a vortex rate sensor, are needed to drive power amplifiers.

Tests were conducted on both pneumatic and water models. Pneumatic models were used to acquire quantitative data, and water models provided flow visualization and qualitative information. A motion-picture film supplement has been prepared in color to provide the reader with flow visualization for various operating conditions and is available on loan. A request card form and a description of the film are found at the back of this paper. Preliminary results of the work are presented in reference 2.

SYMBOLS

B_c control length, normalized to b_s (fig. 2)

B_{cv} width of center-vent duct, normalized to b_s (fig. 2)

B_r receiver-duct width, normalized to b_s (fig. 2)

B_{sb} setback, normalized to b_s (fig. 2)

b_m maneuvering width (fig. 5), m

b_s supply-nozzle width (fig. 2), m

b_t width of throat between input ducts (fig. 2), m

d distance swept by supply jet stream at receiver (fig. 18), m

G_p pressure gain, $\Delta p_o/\Delta p_i$

h_s supply-nozzle depth (fig. 2), m

L_r receiver distance, normalized to b_s (fig. 2)

L_{sp} splitter distance, normalized to b_s (fig. 2)

N_{Re} Reynolds number, based on depth of supply duct, $Q_s/b_s\upsilon$

P_b bias pressure (measured relative to p_{vc}), percent of supply pressure p_s, $\dfrac{p_{i1} + p_{i2}}{2p_s} \times 100$

p_i, p_{i1}, p_{i2} input pressure in an input duct, measured relative to p_{vc}, Pa

Δp_i input differential pressure, Pa

p_o, p_{o1}, p_{o2} output pressure in an output (receiver) duct, Pa

Δp_o output differential pressure, Pa

p_s supply pressure, measured relative to p_{vc}, Pa

p_{vc} vent-chamber pressure, measured relative to return manifold, Pa

Q_i, Q_{i1}, Q_{i2} input flow in an input duct, m^3/sec

ΔQ_i input differential flow, m^3/sec

Q_o, Q_{o1}, Q_{o2} output flow in an output (receiver) duct, m^3/sec

Q_s supply flow, m^3/sec

V_s average velocity in supply nozzle, m/sec

θ supply jet-stream deflection angle (fig. 18), rad

υ kinematic viscosity, m^2/sec

σ aspect ratio of supply duct from reference 5 (fig. 2)

Instability is defined as the variation in the fluid parameters other than noise, for example, more than one operating point due to duct shape, hysteresis effects, or oscillations.

Noise is defined as the unwanted nonperiodic fluctuations in fluid properties, typically generated by flow turbulence, environmental mechanical perturbations, and so forth.

Stability is defined as the constancy of fluid properties (i.e., pressure, flow, etc.) under specified operating conditions.

APPARATUS AND TEST PROCEDURES

Fluidic devices utilize flow phenomena to manipulate fluid signal intelligence which is represented by the fluidic quantities of pressure and flow. Fluid signal intelligence is usually in the form of differential pressures between two parallel signal paths. Many parameters of fluidic devices are analogous with electrical quantities and functions, such as pressure level (voltage), flow (current), flow resistance (electrical resistance), pressure gain (voltage gain), and so forth.

The fluidic amplifiers used in this investigation were proportional; that is, the output differential pressure is proportional to the applied input differential pressure. Such an amplifier (fig. 1) operates as follows: A jet of fluid from the supply nozzle flows through a control interaction region and impinges downstream on two output receiver ducts. A differential pressure applied across the two input ducts causes the supply jet to deflect as it passes through the control interaction region. The deflected jet then impinges more directly on one output receiver duct than the other; this deflection results in a differential output pressure which is proportional to the applied input differential pressure. If no differential input pressure is applied, the supply jet impinges equally on the two output receiver ducts and the differential output pressure is zero. Vents are provided to remove extraneous fluid and prevent unwanted local pressure gradients within the amplifier.

Proportional pressure-controlled pneumatic fluidic amplifiers (ref. 3) were modified for this study by the addition of supply-flow conditioning so as to improve amplifier operation in the laminar-flow region. These amplifiers were then used to determine the effects of design-parameter variations on performance and to study techniques of matching and staging for high overall pressure gain. The parameters varied were aspect ratio σ, setback B_{sb}, control length B_c, splitter distance L_{sp}, receiver-duct width B_r, and width of the center-vent duct B_{cv} (figs. 1 and 2). Table 1 shows the range of dimensional

variations for the amplifier studied. The pneumatic models had a supply-nozzle width of 1 mm and the water models were eight times the size of the pneumatic models.

Water Models

The water models were machined from clear acrylic on a line-tracing milling machine which used line drawings generated by a computer. For the water-model tests (fig. 3), cover and base plates provided a collection manifold for the vents, water connections, dye-trace input connections, and air bleed valves. The amplifier was sandwiched between the cover and base plates and was secured with large clamps. Figure 4 is a functional schematic of the test setup for water-flow visualization. In order to maintain constant supply-pressure conditions and to minimize undesirable aeration, water was pumped up to a constant-level supply tank from a large settling tank. The water then flowed through a test model to the constant-level drain tank. Three flow meters between the supply tank and the test model monitored supply flow and each input flow. The supply stream (red) and each input stream (blue and yellow) were tinted with a different color dye to aid visualization of flow phenomena. Provisions were also made to tag individual streamlines in the supply flow with dark green-dye traces (figs. 4 and 5). Alcohol was added to the dye to compensate for the higher density of the dye trace in the water (ref. 4).

The large transparent water models provided an excellent method of visualizing complex flow phenomena of fluidic amplifiers. Some parameter variations produce easily observed changes in flow which are clearly shown in the color film supplement. Other characteristics, however, such as gain changes, are not readily observable and must be determined by other means. The pneumatic models were used for quantitative investigations.

Pneumatic Models

The pneumatic models were machined on a pantograph milling machine, using the water models as templates. Figure 6 is a functional schematic of pneumatic-model tests and shows pressure and flow test points. The test instrumentation included pressure transducers (capacitance type), flow meters (laminar-flow tubes), and a fluidic signal generator. Supply and input pressures were measured relative to vent-chamber pressure, and output and vent-chamber pressures were measured relative to ambient pressure. The flows Q_s, Q_{i1}, Q_{i2}, Q_{o1}, and Q_{o2} were also monitored. All of the vents of the test amplifier were vented to a common collection manifold (vent chamber) contained in the test cover block shown in figure 7. The vent chamber was vented to atmosphere through a variable restrictor valve used to set and control vent-chamber pressure. Input and output differential pressures were recorded on an x-y plotter to measure gain.

In setting up the pneumatic-model tests, output flow was adjusted by means of the output restrictor valves to simulate the loading effect which would be presented by a following amplifier stage. The fluid signal generator was then used to adjust the input-duct steady-state pressure (i.e., the pressure in the

input duct with no differential input pressure applied) with the vent chamber opened to atmosphere to simulate the pressure and flow effects of a previous amplifier stage. The average of the steady-state pressures of the two input ducts with no differential input pressure applied is hereinafter referred to as the bias pressure. The restrictor valve on the vent-chamber exhaust line was then adjusted to set the bias pressure to the same pressure as the vent-chamber pressure. The signal generator is a device which generates a differential pressure and allows independent variation of bias pressure and differential pressure. Amplifier pressure gain was determined by varying the differential pressure of the ducts and measuring the output differential pressure while the bias pressure was held constant by the signal generator. The signal generator was then set to a different bias pressure, and gain was replotted. Data were collected for bias pressures of 0 percent, ±5 percent, and ±10 percent of supply pressure.

DISCUSSION AND RESULTS

Reynolds Number

Reynolds number is a nondimensional number characteristic of the flow of a fluid in a channel or past an obstruction. As used in this paper, it is analogous to pipe flow where the supply-nozzle depth h_s (fig. 2) is used as the characteristic dimension. (See ref. 1.) As shown in equation (1), the Reynolds number N_{Re} at the supply nozzle is the product of the average velocity of the supply flow through the nozzle V_s and the nozzle depth h_s, divided by the kinematic viscosity υ; that is,

$$N_{Re} = \frac{V_s h_s}{\upsilon} \tag{1}$$

The supply flow Q_s is expressed as the product of the cross-sectional area of the supply nozzle ($b_s h_s$) and the average supply velocity V_s; that is,

$$Q_s = b_s h_s V_s \tag{2}$$

which can be rewritten as

$$h_s V_s = \frac{Q_s}{b_s} \tag{3}$$

Equation (3) can be substituted into equation (1) to yield

$$N_{Re} = \frac{Q_s}{b_s \upsilon} \tag{4}$$

which is a more convenient form. A typical plot of pressure gain as a function of Reynolds number for a pneumatic amplifier is presented in figure 8, from which it can be seen that pressure gain peaks at a Reynolds number of approximately 800 and thereafter slowly decreases with Reynolds number. Noise also

increases as Reynolds number increases. Photographs of the flow fields found in the fluidic amplifier for several Reynolds numbers are presented in figure 9. At $N_{Re} = 250$, the flow is very quiet (fig. 9(a)) and the pressure gain is low (fig. 8); at $N_{Re} = 800$, the flow is quiet (fig. 9(b)) and the pressure gain is near maximum (fig. 8); and at $N_{Re} = 1600$, the supply stream is turbulent (fig. 9(c)) and very noisy.

Aspect Ratio

The aspect ratio σ of a fluidic amplifier is the ratio of supply-nozzle depth h_s to supply-nozzle width b_s (fig. 2). If amplifiers of the same plan-view silhouette but of different supply-duct depths (i.e., different aspect ratios) are operated at the same Reynolds number N_{Re}, the gain, flow, and bias properties of the amplifiers are essentially the same; however, the required operating pressures will differ. For example, an amplifier with a supply duct of 1.5-mm depth and 1-mm width ($\sigma = 1.5$) can be operated at a supply pressure of 133 Pa, whereas an amplifier with a supply duct of 0.3-mm depth and 1-mm width ($\sigma = 0.3$) would require a supply pressure 50 times greater to operate at the same Reynolds number.

Bias Pressure

Bias pressure P_b is the average pressure of the two input control ducts expressed as a percentage of the supply pressure p_s; that is,

$$P_b = \frac{p_{i1} + p_{i2}}{2p_s} \times 100 \tag{5}$$

Bias pressure affects the gain, stability, and noise level of a fluidic amplifier. Pressure gain as a function of bias pressure is plotted in figure 10; this typical plot shows that high positive bias pressure reduces gain and that low bias pressure reduces stability. As bias pressure is reduced, gain usually increases until an unstable condition is reached, but a maximum gain may occur before the unstable condition is reached. It can be seen from figure 11(a) that the supply stream (red) is squeezed in as the high bias flow (blue and yellow) from the controls spills through the throat at the downstream edge of the controls. Figure 11(b) shows two tagged streamlines (green) in the supply flow for a large negative bias condition. The flow in the control ducts is negative and moves out through the input control ducts. The flow is unstable in the center position, that is, in a flip-flop condition, and the photograph (fig. 11(b)) was taken as the supply stream switched from one output to the other.

Vent-Chamber Pressure

The vent chamber collects all of the flow from the various vents of an amplifier and exhausts this flow to the low-pressure return line through a variable restrictor valve, which thereby sets and controls the vent-chamber pressure p_{vc}. If the vent-chamber pressure is increased by restricting exhaust flow,

bias pressure P_b is decreased and amplifier gain is affected, which was noted previously and illustrated in figure 10. Controlling amplifier gain with vent-chamber pressure was found to be very convenient.

Setback and Input Resistance

Setback B_{sb} is the distance between the downstream edge of an input duct and an ideal, nonexpanded, centered supply jet stream. Setback is normalized to supply-nozzle width b_s (fig. 2) and is calculated from the following equation:

$$B_{sb} = \frac{b_t - b_s}{2b_s} \tag{6}$$

Maneuvering width b_m (fig. 5) is the width between the downstream edge of the input duct and a real supply jet stream. Maneuvering width is the significant parameter under investigation, rather than the parameter B_{sb} (width for an ideal supply jet stream). However, maneuvering width is impractical to determine because of the difficulties of accurately measuring or calculating the width of the real supply jet stream. Therefore, setback B_{sb} is ordinarily used to make comparative measurements in practical applications.

Setback and bias pressure are two important parameters which affect the input impedance of fluidic amplifiers. The usually employed term "input impedance" is a complex concept. (See ref. 5.) For the purposes of the present paper, the input-impedance parameter is taken as the resistance to input-duct flow (input resistance) and is expressed as the ratio of Δp_i to ΔQ_i. Setback affects amplifier bias, gain, gain-saturation characteristics, and input-impedance characteristics. As B_{sb} is reduced, pressure gain increases, as shown in figure 12, but gain-saturation characteristics deteriorate, as described subsequently.

Fluid resistance is indicated by the slope of the curve generated by plotting input pressure p_i as a function of input flow Q_i. The slopes of the curves in figure 13 illustrate changes in input-duct flow resistance for two setback dimensions $B_{sb} = 0.063$ (purple curve) and $B_{sb} = 0.625$ (blue curve). The smaller value of setback allows less input flow, that is, higher input resistance (slope of purple curve), than the larger value of setback (slope of blue curve). The slopes of the blue and purple curves show the input resistance to bias flow; this resistance is the jet-centered or undeflected input resistance generated by keeping the input differential pressure Δp_i equal to zero. The shorter intersecting curves (red and green) of constant-bias pressure are examples of flow-resistance characteristics generated by keeping bias pressure constant in the two input ducts and by varying the differential pressure between them. The differential-pressure variation deflects the supply jet stream, thereby causing a less restrictive path for the input flow. This effect can be seen in figure 14, which shows a deflected supply stream. The less restrictive path is shown by the increased width of the blue control path between the supply stream and the downstream edge of the control. Figure 13 illustrates two important characteristics of input resistance. First, the resistance to signal flow,

indicated by the slopes of the red and green curves, is less than the resistance to bias flow, indicated by the slopes of the blue and purple curves; and second, as bias pressures are increased, the resistance to signal flow decreases only slightly, as indicated by comparing (for a particular setback) the slope of a green curve to the slope of a red curve. The pressure and flow in the control ducts can be negative.

Since the setback dimension affects pressure-gain characteristics, the selection of a setback dimension depends on the intended amplifier application. Figure 15 shows three conceptual pressure-gain curves which include saturation regions (where the differential output pressure Δp_o no longer increases directly with increasing input differential pressure Δp_i). If the application allows gain saturation, it is usually desirable for Δp_o to remain at, or close to, maximum, as shown in the conceptual curve of figure 15(a). Such a gain-saturation characteristic would be obtained at the higher values of setback, such as $B_{sb} = 0.625$ to $B_{sb} = 1.0$. However, as setback is reduced to produce higher pressure gain, the gain-saturation characteristic deteriorates, as shown conceptually in figure 15(b). Differential output pressure after saturation is reduced because the supply stream is deflected off the downstream edge of the input duct, as shown visually in figure 16 and in the film supplement. An example of a saturation characteristic for an extremely low setback is shown conceptually in figure 15(c). Pressure gain is very high in the linear region, but the output signal Δp_o reverses polarity in gain saturation and is unstable in a manner probably not useful for any application. The instability of the pressure-gain characteristics of figure 15(c) occurred at low bias pressures which produced negative flow in one or both of the input ducts and caused the supply jet stream to impinge upon the downstream edge of the input duct.

Control Length

Control length B_c (fig. 2) is the distance from the supply nozzle to the throat, that is, the downstream edge of the input duct. Increasing the control length increases the area over which the input pressure acts, thus producing greater deflection force. Increasing the normalized control length B_c from 1.25 to 5.25 increases gain, as shown in figure 17.

However, increasing the control length decreases maneuvering width b_m, which is shown as the clearance between the supply stream and the downstream edge of the input duct in figure 5. Decreased maneuvering width adversely affects gain-saturation characteristics of the amplifier. Increased maneuvering width is required for jet deflection if larger control lengths are employed. Additional maneuvering width is achieved by increasing setback, which, however, decreases gain and input resistance.

Splitter Distance

Splitter distance L_{sp} (fig. 2) is the distance from the supply-duct nozzle to the receiver ducts. There are two opposing factors to be considered in choosing splitter distance. First, amplifier gain increases with normalized splitter distance L_{sp} because sweep distance d (fig. 18) increases with

splitter distance L_{sp} for any particular supply jet-stream deflection angle θ. The opposing consideration is the spreading and slowing of the supply jet stream as it proceeds downstream. Figures 19(a) and 19(b) conceptually illustrate differences in output-pressure profiles as a function of sweep distance for two amplifiers having different splitter distances. Longer splitter distance requires greater sweep distances for equal output-pressure increments. Optimum gain as a function of normalized splitter distance L_{sp} was found to occur at approximately nine. (See fig. 20.)

Receiver-Duct Width

The process of determining receiver-duct width (fig. 2) involves several trade-offs. The pressure at the receiver duct is the average of the impinging pressure profile of the supply jet. As shown in figure 21, narrower receiver-duct widths produce higher gain. However, narrower receiver ducts also have higher resistance to flow. Thus, if larger output flow is required for a low input resistance to a following stage or load, a wider receiver-duct width for low effective output resistance is required. Practical considerations in choosing small duct widths are fabrication and susceptibility to disturbances in operation caused by contamination.

Width of Center-Vent Duct

Figure 22 shows that pressure gain decreases with increasing width of center-vent duct B_{cv}. Extrapolation of figure 22 implies that highest gain would be realized with no center vent, but this is not the case in actual practice (refs. 5 and 6). The center-vent configuration was chosen for this study to obtain lower average output pressures at the receivers to facilitate cascading stages. This is desirable because the bias pressure at the input of a cascaded-amplifier stage is the output of the preceding stage. Thus, it may be advantageous to minimize the average output pressure of intermediate stages by employing center vents to remove a portion of the midstream flow when cascading stages. The value $B_{cv} = 0.75$ was chosen for the working models of this study as a practical trade-off among gain, fabrication, and susceptibility to duct blockage by contamination.

Supply-Flow Conditioning

Supply-flow conditioning was used in this investigation of fluidic-amplifier performance to minimize flow perturbations caused by variations in the incoming supply fluid. Supply-flow conditioning was accomplished by the long section of flow straighteners (fig. 1), followed by a converging section of duct where the flow was rapidly accelerated to the supply nozzle.

Cascading Amplifiers for High Overall Pressure Gain

As noted in the introduction, one of the objectives of this study was to investigate improvement of techniques of cascading, proportional fluidic ampli-

fiers for high overall pressure gain. It is important that a high-pressure-gain amplifier operate in laminar flow to minimize the noise interference associated with turbulent flow, which can substantially reduce the threshold sensitivity of low-level output devices such as a vortex rate sensor. The choices of proper aspect ratio and vent-chamber pressure were found to be fundamentally important for cascading, multistage fluidic amplifiers in order to obtain high overall pressure gain.

In this study, five stages of laminar-flow amplifiers with the same plan view were cascaded for high overall pressure gain. Each successive stage had a lower aspect ratio and a higher supply pressure, which resulted in all stages operating at approximately the same Reynolds number, with adequate stage-to-stage impedance matching.

Each amplifier stage had an individual vent chamber and variable restrictor valve which allowed its vent-chamber and bias pressures to be controlled independently of other stages. This technique permitted the cascaded-amplifier bias pressures to be set for the desired high end-to-end pressure gain and, at the same time, provided for interstage impedance match "tuning" for best overall performance (ref. 7). In effect, the adjustable vent-chamber restrictors allow the operating point of each stage of the amplifier to be set at the optimum trade-off point between high gain and stability.

Five individual amplifiers (like the one shown in fig. 7) were staged together to yield a stable overall pressure gain slightly in excess of 2 000 000. These five amplifiers were driven by a constant-bias fluidic signal generator and fed into a blocked-output load (i.e., no output flow but high output pressure); gain could be adjusted to a peak of about 2 250 000, but a slight reduction in gain provided more stable operation. Five amplifiers of identical plan-view silhouette were integrated into a single block and are shown in figure 23. Supply and vent manifolds were cast into the block with provisions for attaching supply and vent-chamber adjustment restrictors. This configuration, driven by a vortex rate sensor, produced an overall pressure gain of 100 000 when driving a pair of diaphragms (blocked load). Higher useful gains could be realized in other applications. The nominal supply pressures for the five stages were 113 Pa, 500 Pa, 1000 Pa, 2000 Pa, and 6000 Pa; and aspect ratios for the 1-mm-wide supply-duct nozzles were 1.5, 0.75, 0.5, 0.375, and 0.3, respectively.

CONCLUDING REMARKS

A study has been made of the effects of dimensional and operating-condition variations on performance characteristics of proportional laminar-flow jet-deflection fluidic amplifiers. Dimensions and operating conditions were varied one at a time to determine the characteristic changes attributable to each parameter. Aspect ratio and vent-chamber pressure were found to be the two most important parameters affecting the multistage performance of these amplifiers.

It was found that there is an optimum Reynolds number for maximum gain for a specific design of a laminar-flow proportional amplifier. In order to accommodate different supply pressures, the aspect ratio can be changed to maintain a

constant Reynolds number. Pressure gain as a function of bias level was found to be controllable with vent-chamber pressure. Increasing the setback dimension reduced gain and resistance to input bias flow and improved gain-saturation characteristics. Increasing control length increased gain but adversely affected gain saturation. The optimum splitter distance was found to be approximately nine times the supply-duct width. Pressure gain was found to increase with decreasing width of center-vent duct. Decreasing receiver-duct width increased gain but also increased output resistance. Independent adjustment capability of vent-chamber pressure in each stage is important for high overall pressure gain of multistage fluidic amplifiers and permits impedance matching and optimization. In effect, the adjustable vent-chamber restrictors allow the operating point of each stage of the amplifier to be set at the optimum trade-off point between high gain and stability. Five pneumatic fluidic amplifiers were staged together and were found to yield stable overall pressure gain slightly in excess of 2 000 000. The findings and data of this study should be a useful guide for the design, construction, and operation of proportional laminar-flow fluidic amplifiers.

Langley Research Center
National Aeronautics and Space Administration
Hampton, VA 23665
July 8, 1977

REFERENCES

1. Kirshner, Joseph M.; and Manion, Francis M.: The Jet-Deflection Proportional Amplifier. 70-Fics-17, American Soc. Mech. Eng., June 1970.

2. Hellbaum, R. F.: Experimental Design of Laminar Proportional Amplifiers. Fluidics Technology, J. M. Kirshner, ed., AGARD-AG-215, Jan. 1976, pp. 209-227.

3. Griffin, William S.; and Gebben, Vernon D.: A Proportional Fluid Jet Amplifier With Flat Saturation and Its Application to Gain Blocks. NASA TM X-1915, 1969.

4. Spyropoulos, Chris E.: Fluerics 36 Large-Scale Modeling of Laminar Flueric Devices. HDL-TM-73-28, U.S. Army, Feb. 1974.

5. Manion, Francis M.; and Drzewiecki, Tadeusz M.: Analytic Design of Laminar Proportional Amplifiers. Fluidics Technology, J. M. Kirshner, ed., AGARD-AG-215, Jan. 1976, pp. 157-207.

6. Manion, Francis M.; and Mon, George: Fluerics: 33. Design and Staging of Laminar Proportional Amplifiers. HDL-TR-1608, U.S. Army, Sept. 1972. (Available from DDC as AD 751 182.)

7. Garner, Howell D.; and Hellbaum, Richard F.: Fluid Pressure Amplifier and System. U.S. Pat. 3,770,021, Nov. 6, 1973.

TABLE 1.- RANGE OF DIMENSIONAL VARIATIONS FOR AMPLIFIER PARAMETERS NORMALIZED TO b_s

[b_s = 1 mm for pneumatic models; b_s = 8 mm for water models]

Aspect ratio, σ	0.25, *0.5, 0.75, 1.0
Setback, B_{sb}	0, 0.063, 0.125, 0.25, *0.375, 0.625
Control length, B_c	1.25, 2.25, *3.25, 4.25, 5.25
Splitter distance, L_{sp}	8.3, *9.3, 10.3, 11.3, 12.3
Receiver-duct width, B_r	0.65, 0.8, *1.0, 1.5
Width of center-vent duct, B_{cv}	0.65, *0.75, 0.85, 1.0

*Value about which other parameters were varied one at a time.

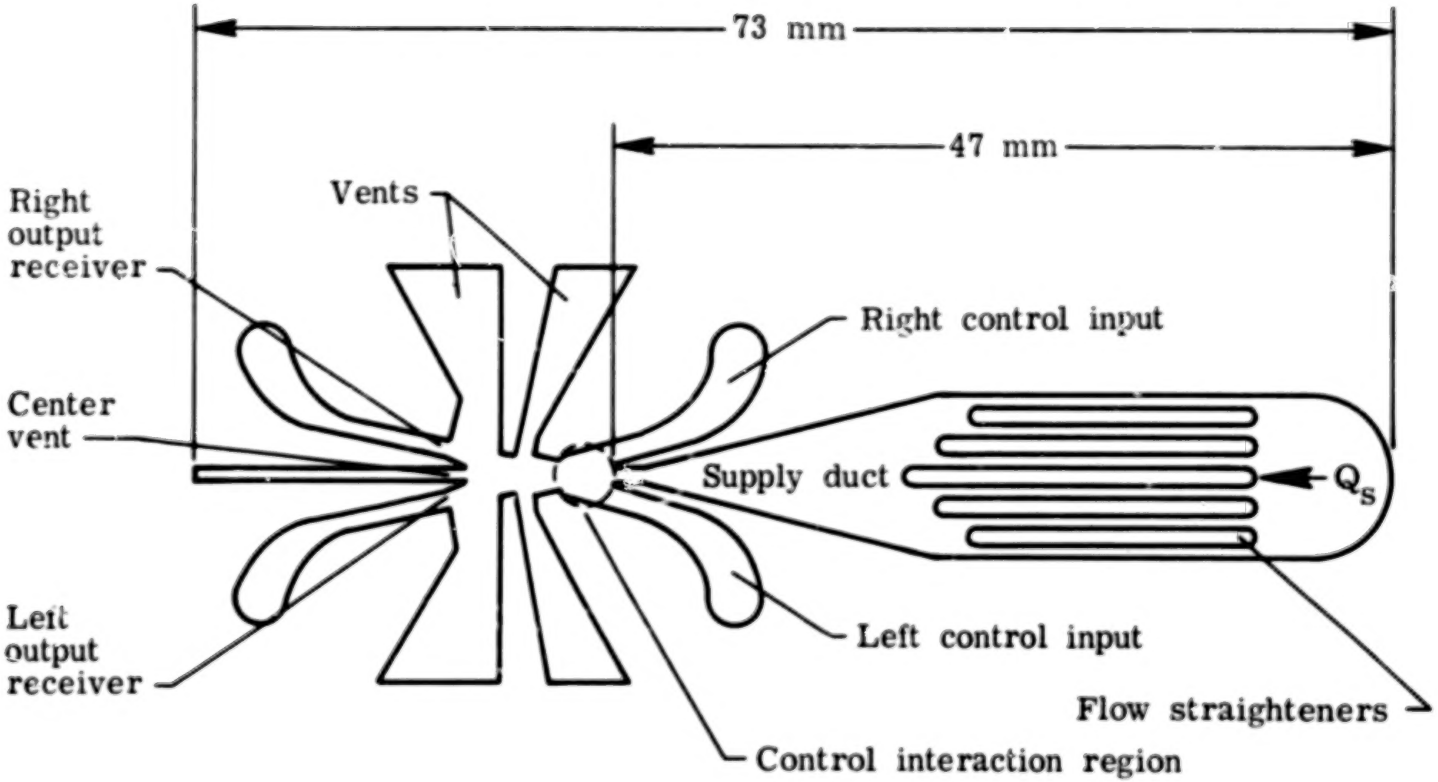

Figure 1.- Pneumatic fluidic amplifier.

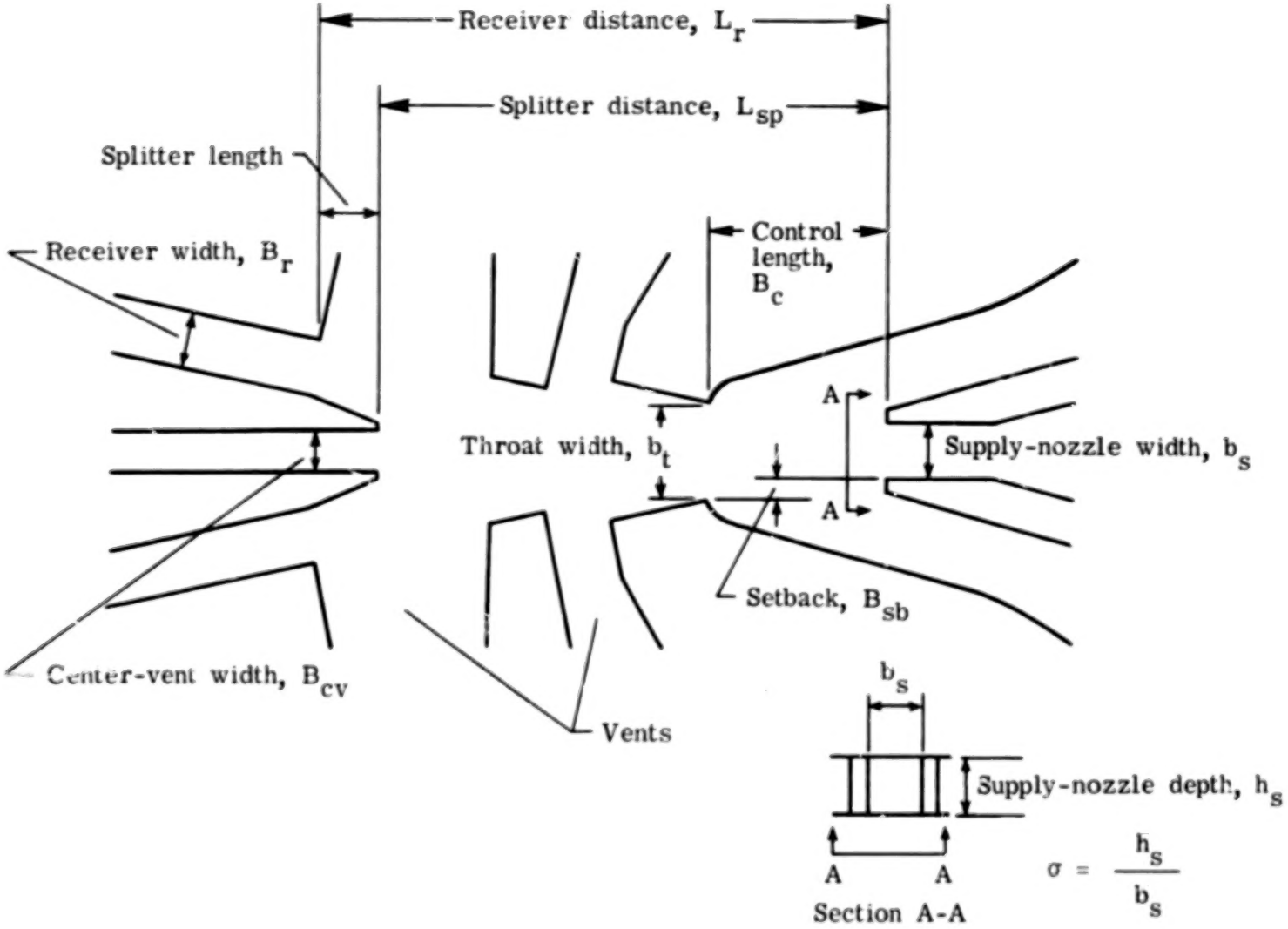

Figure 2.- Amplifier parameters.

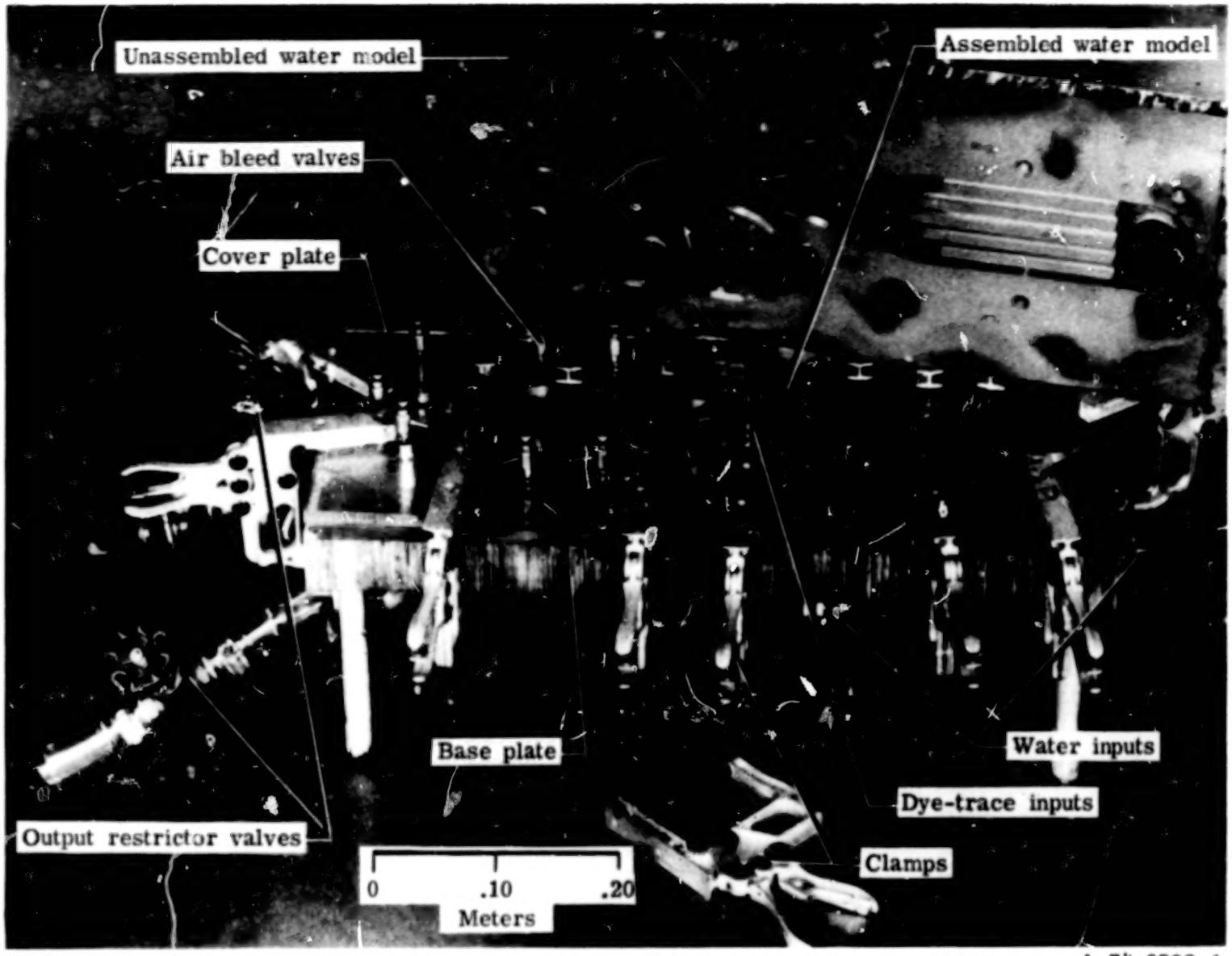

L-74-3522.1

Figure 3.- Two water models.

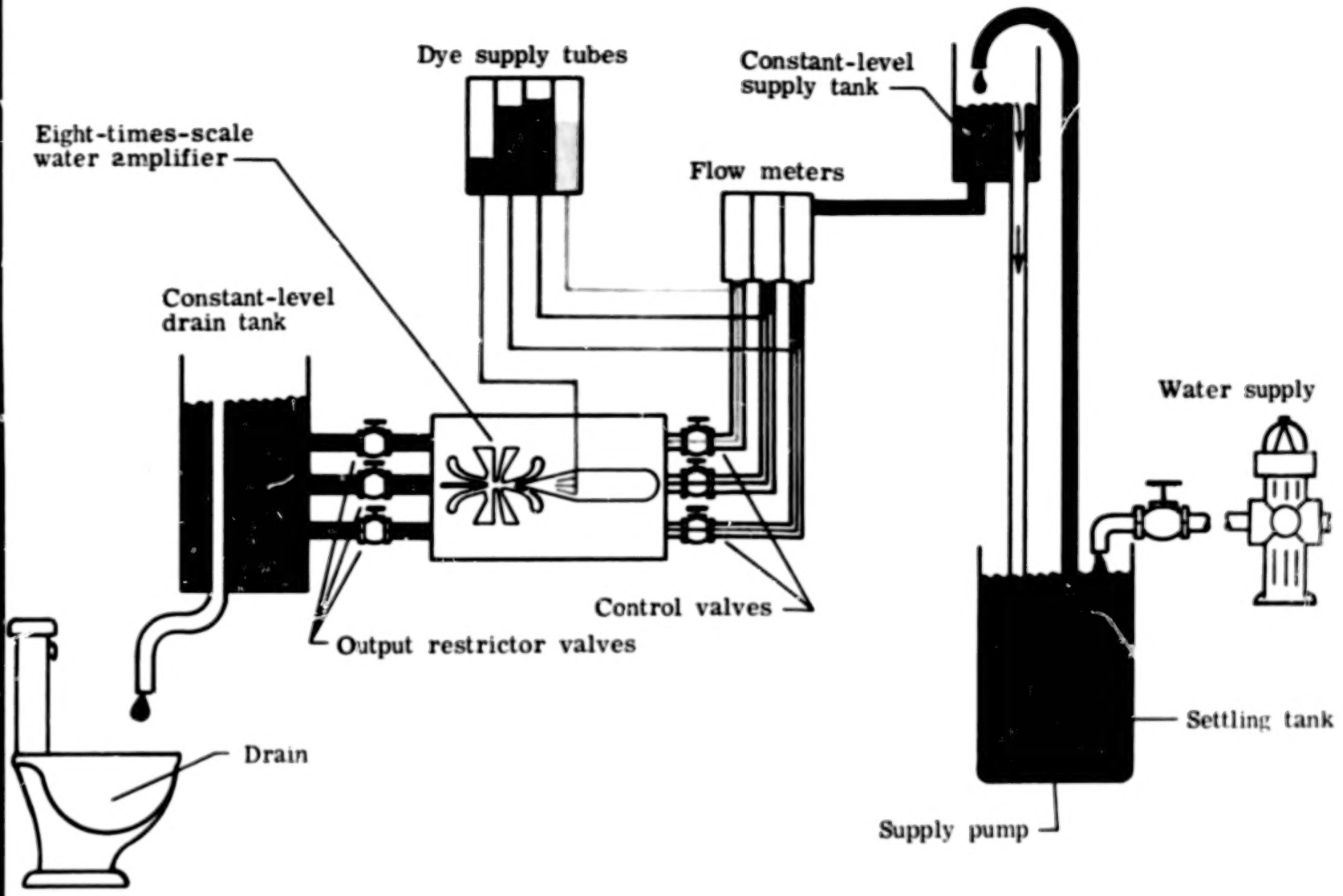

Figure 4.- Functional schematic for water-flow visualization.

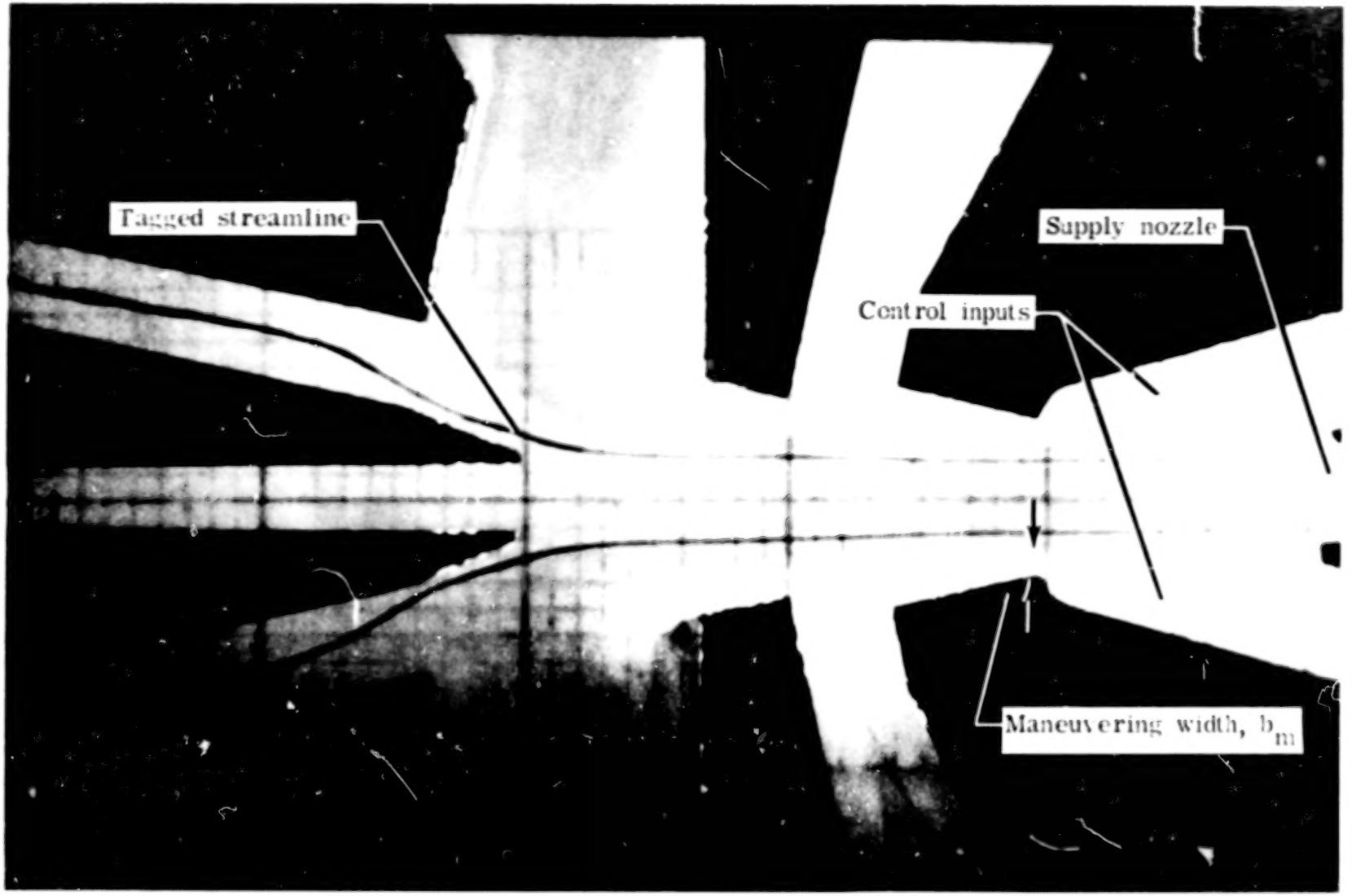

L-77-243

Figure 5.- Water model with tagged streamlines in supply flow.

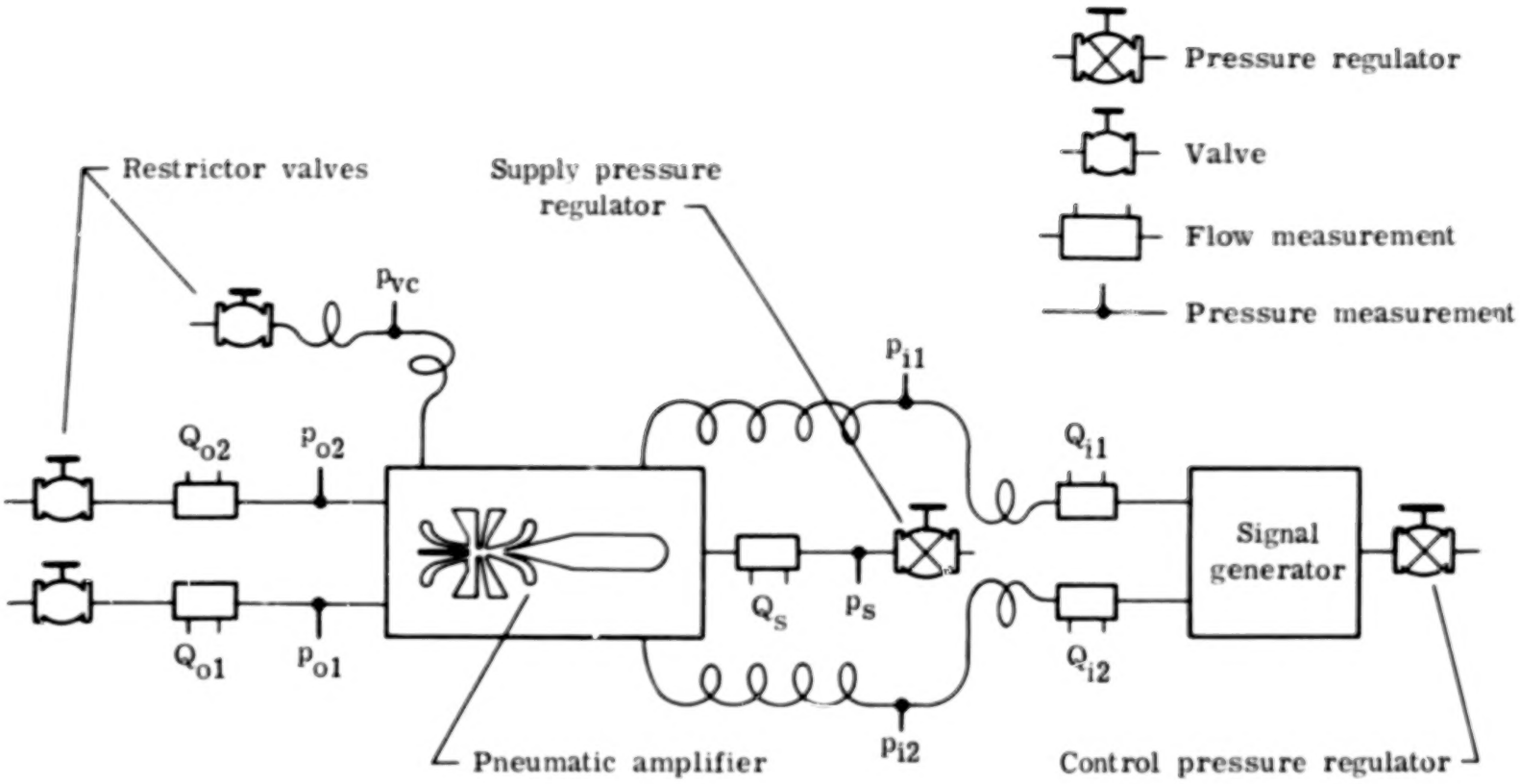

Figure 6.- Functional schematic for pneumatic-model tests.

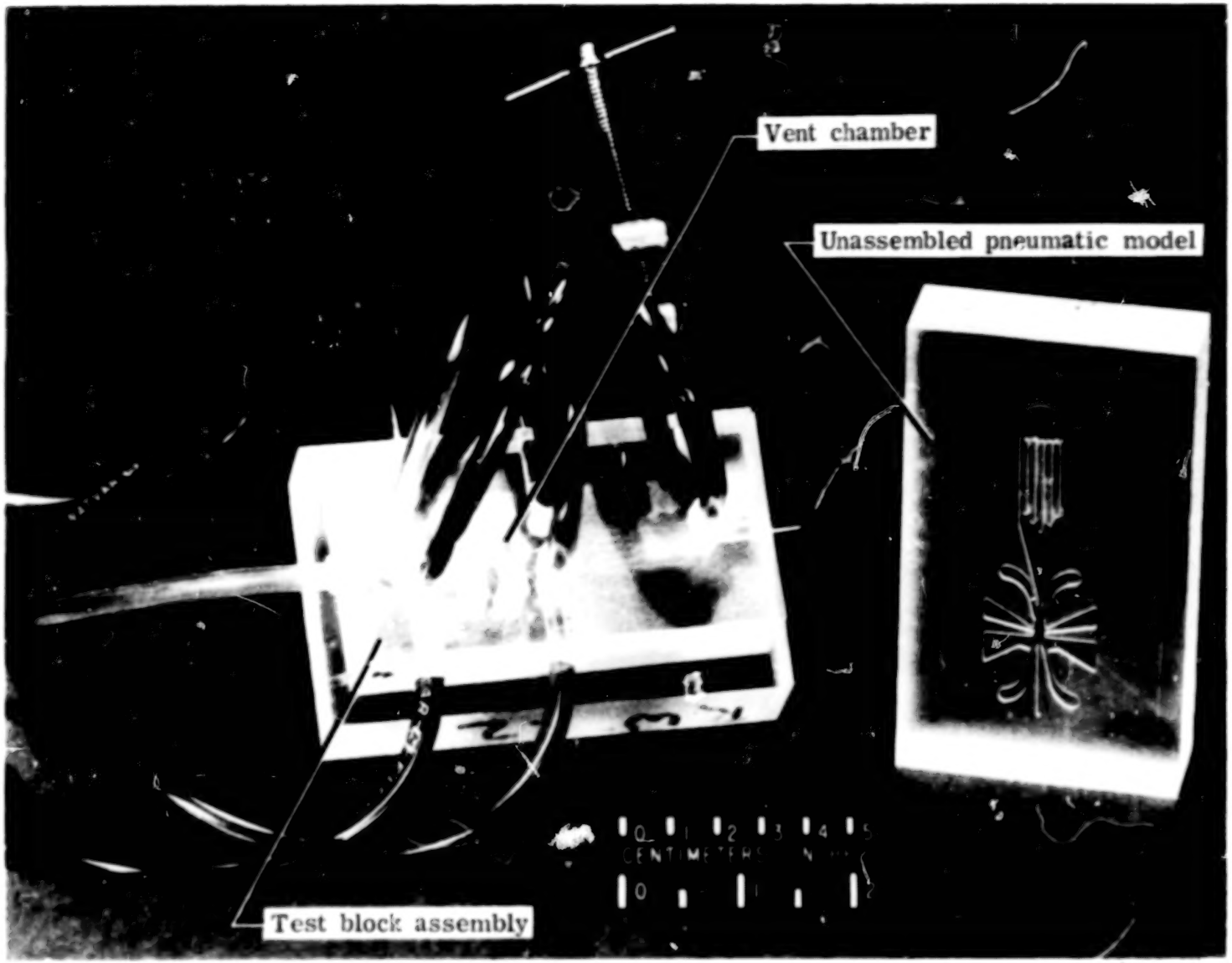

L-74-3523.1

Figure 7.- Two pneumatic models. One assembled with test cover block.

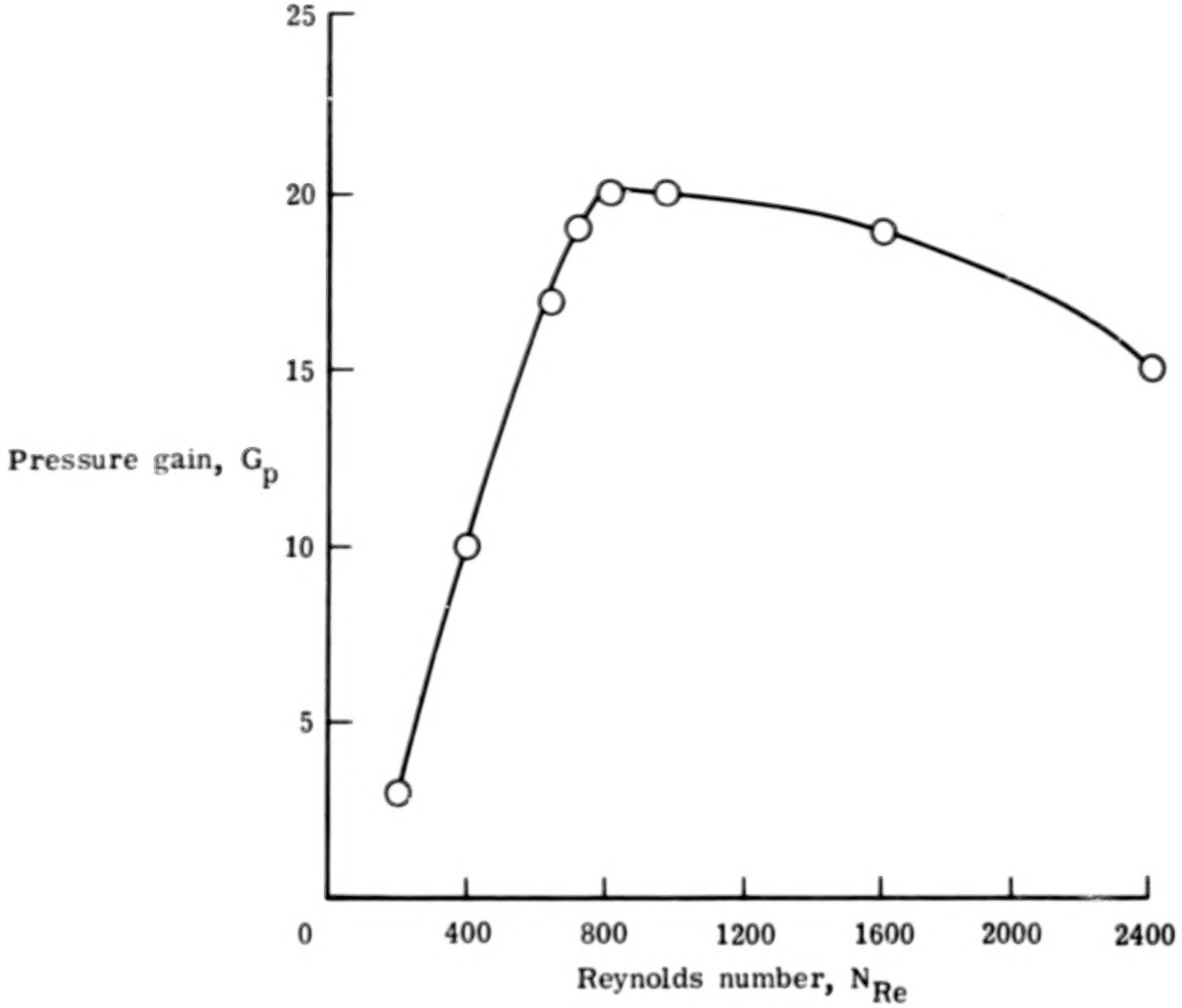

Figure 8.- Pressure gain as a function of Reynolds number. $\sigma = 0.75$.

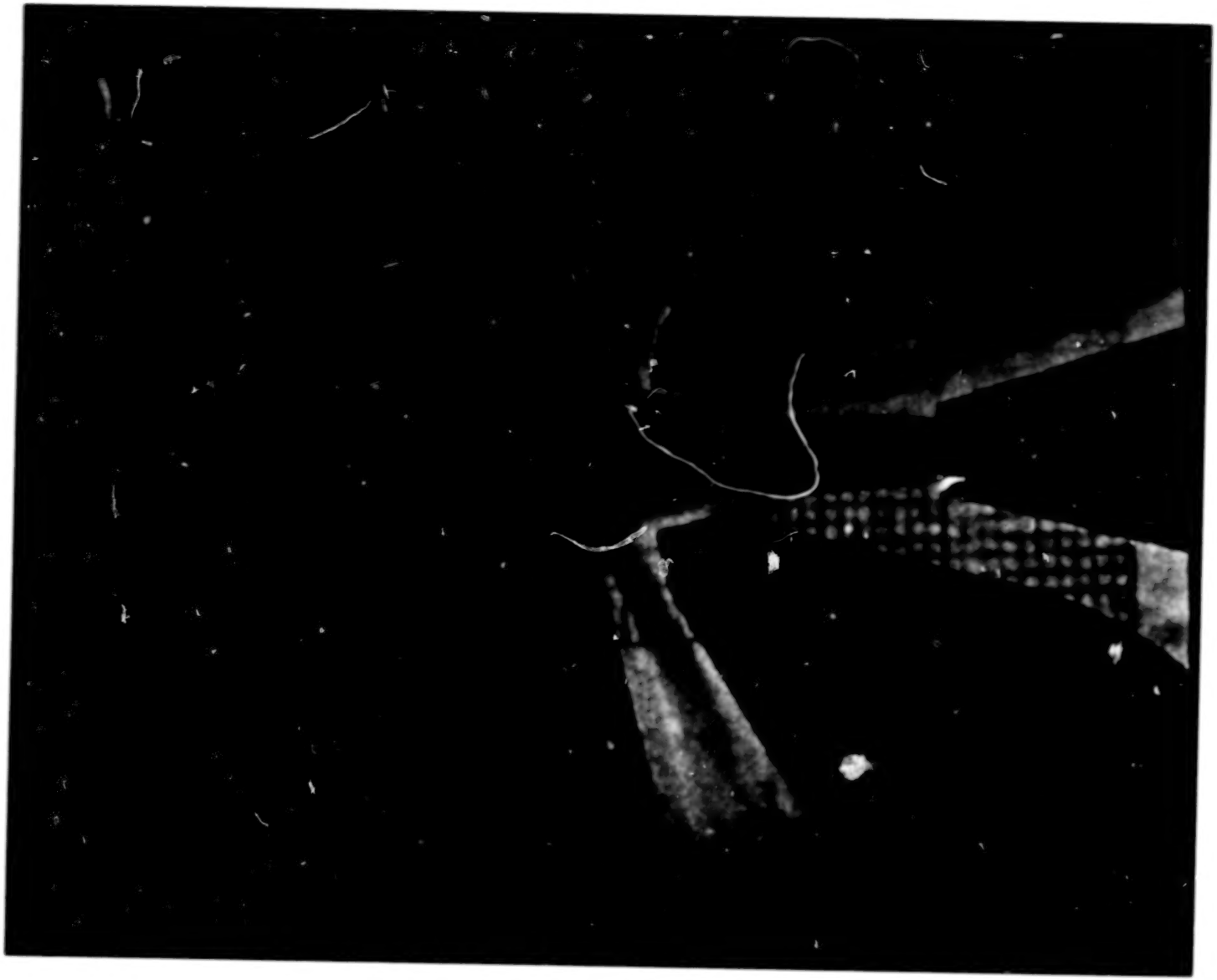

L-77-244

(a) N_{Re} = 250.

Figure 9.- Flow fields in the fluidic amplifier for Reynolds numbers of 250, 800, and 1600.

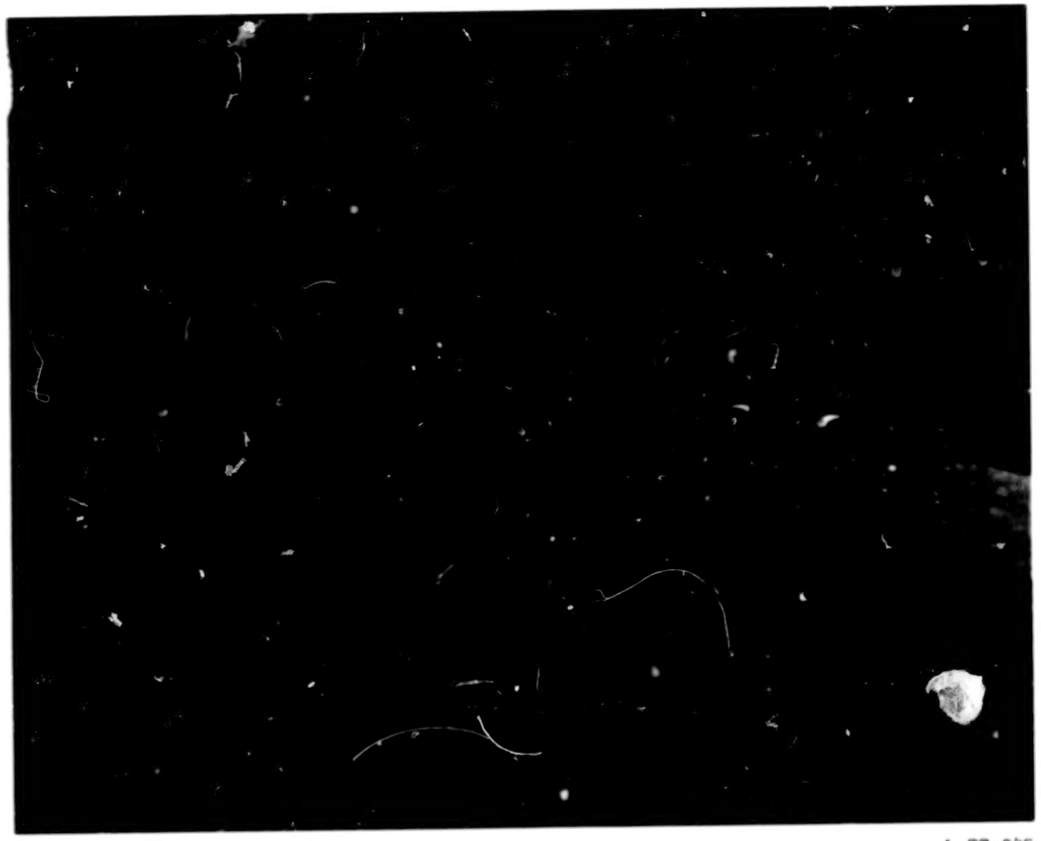

L-77-245

(b) N_{Re} = 800.

Figure 9.- Continued.

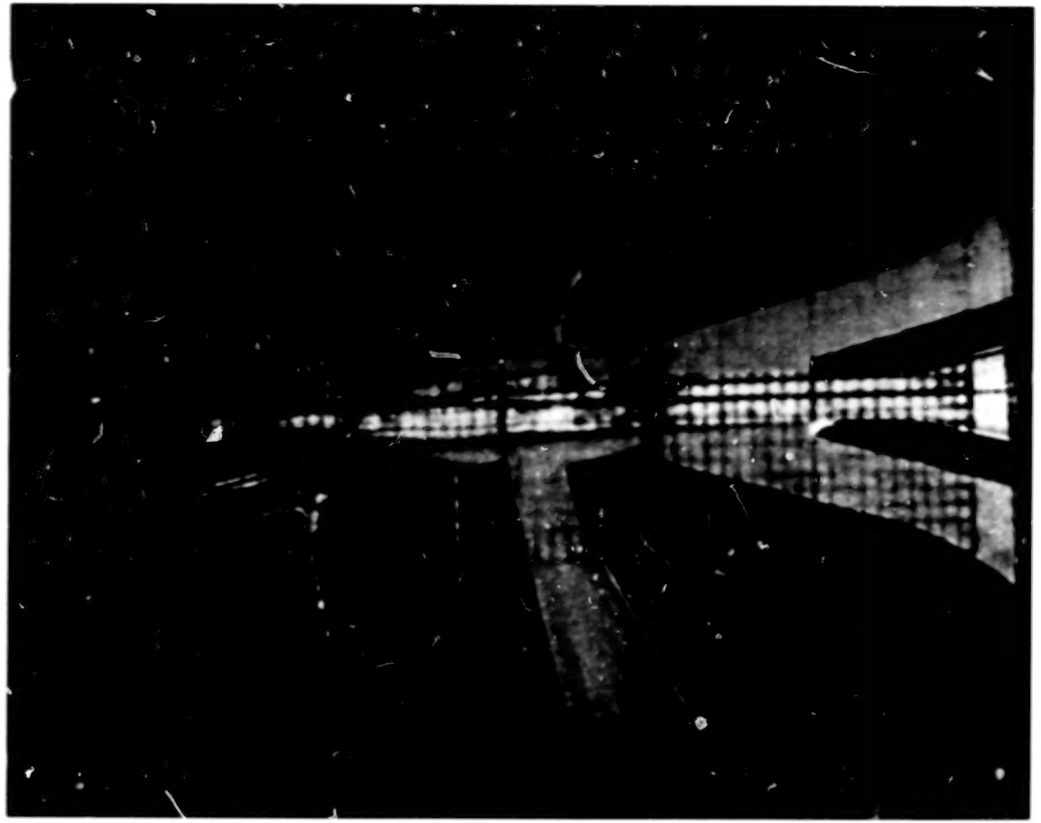

(c) N_{Re} = 1600. L-77-246

Figure 9.- Concluded.

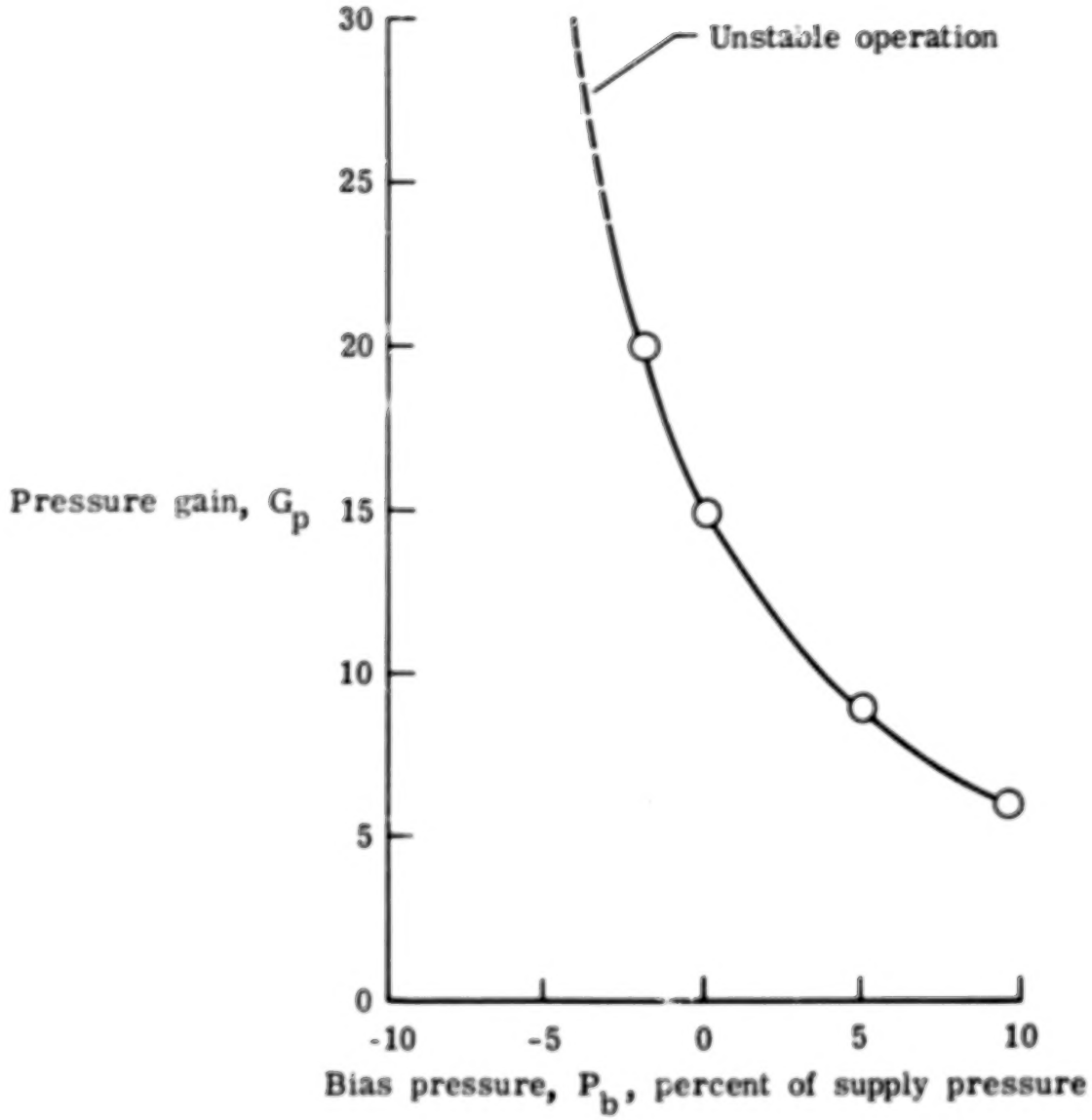

Figure 10.- Pressure gain as a function of bias pressure. $\sigma = 1.5$.

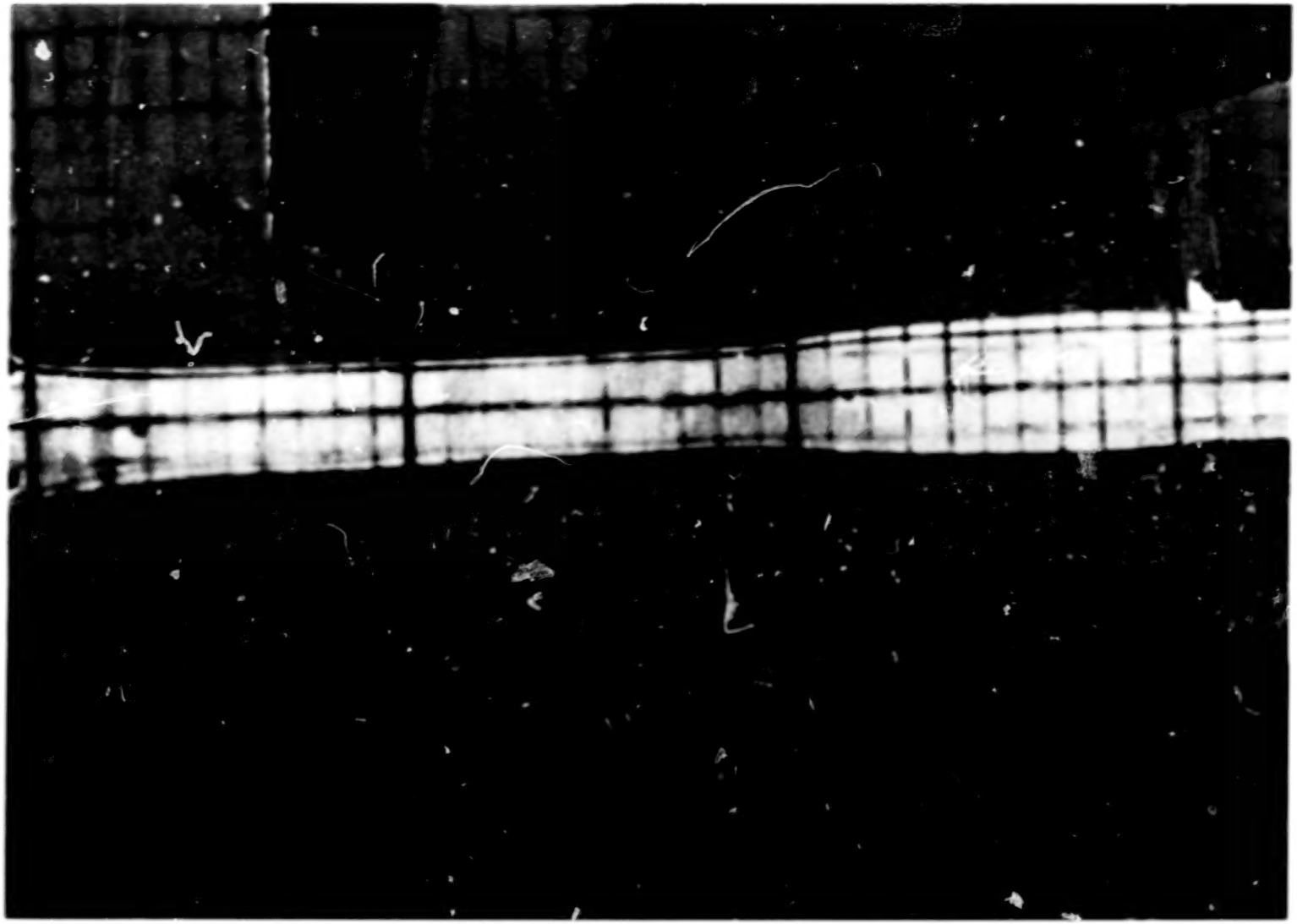

L-77-247

(a) High bias condition.

Figure 11.- Flow fields in the fluidic amplifier for high and low bias conditions.

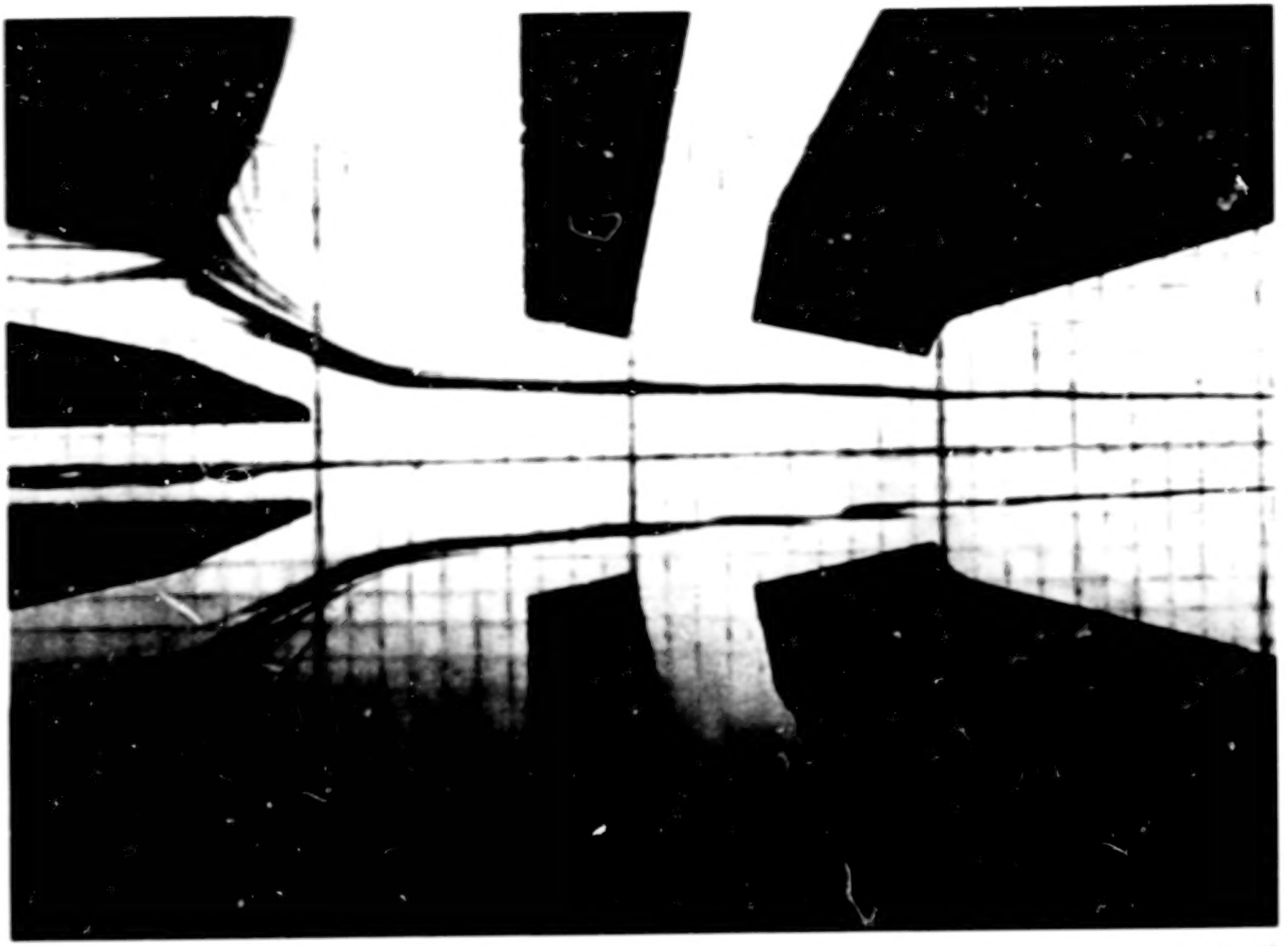

L-77-248

(b) Low bias condition. (Negative bias with control flow moving out through control ducts.)

Figure 11.- Concluded.

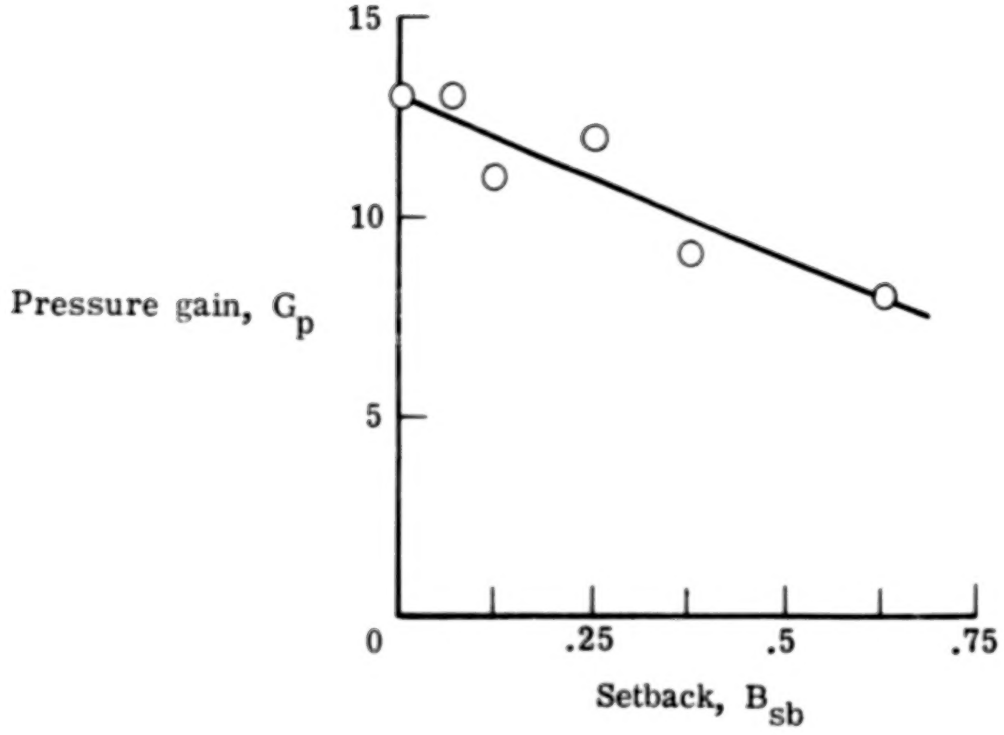

Figure 12.- Pressure gain as a function of setback. N_{Re} = 800; P_b is 5 percent of p_s.

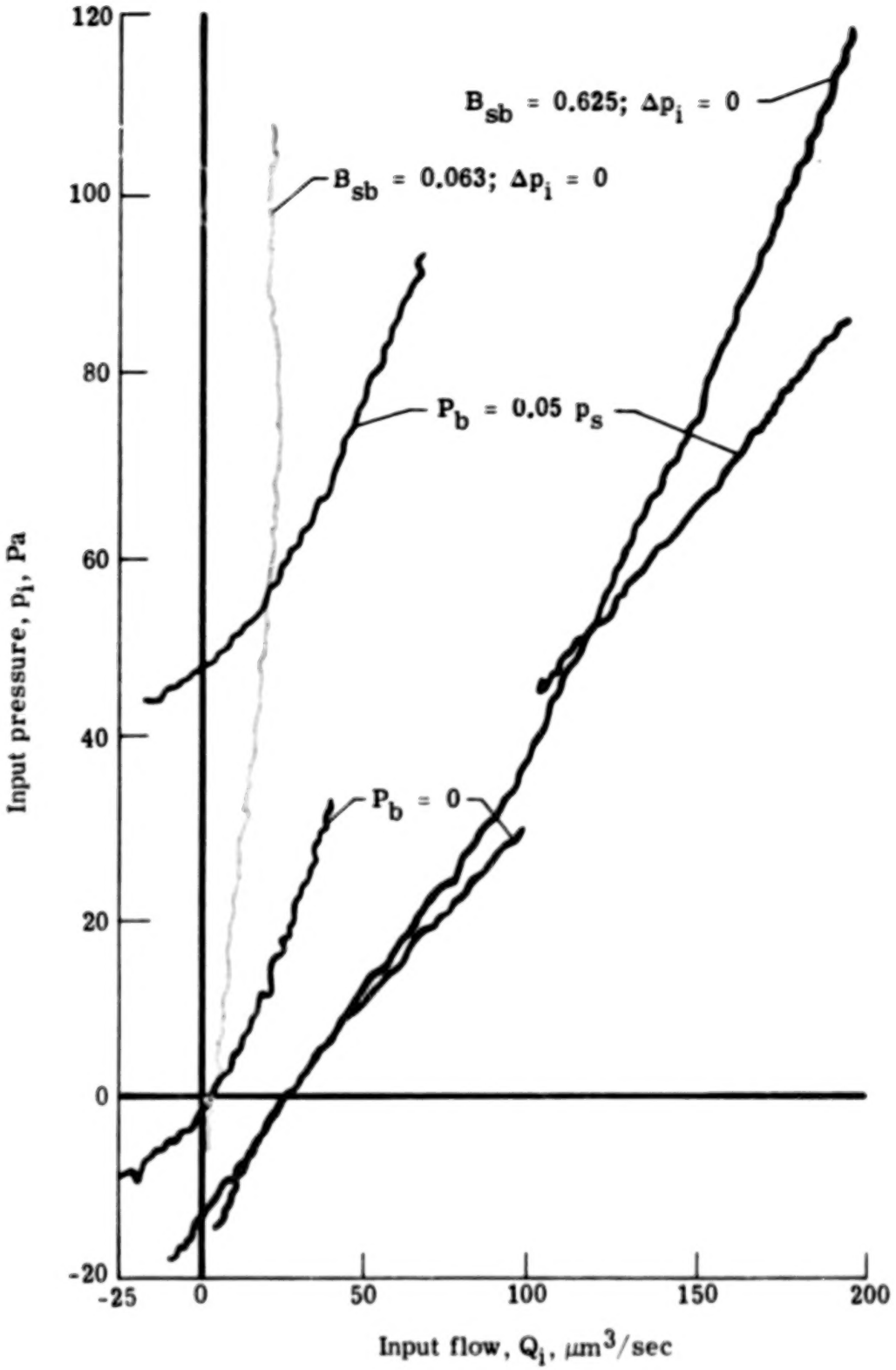

Figure 13.- Input characteristics of two amplifiers (B_{sb} = 0.063 and 0.625) for both constant signal (Δp_i = 0) and constant bias pressure (P_b = 0 and 5 percent).

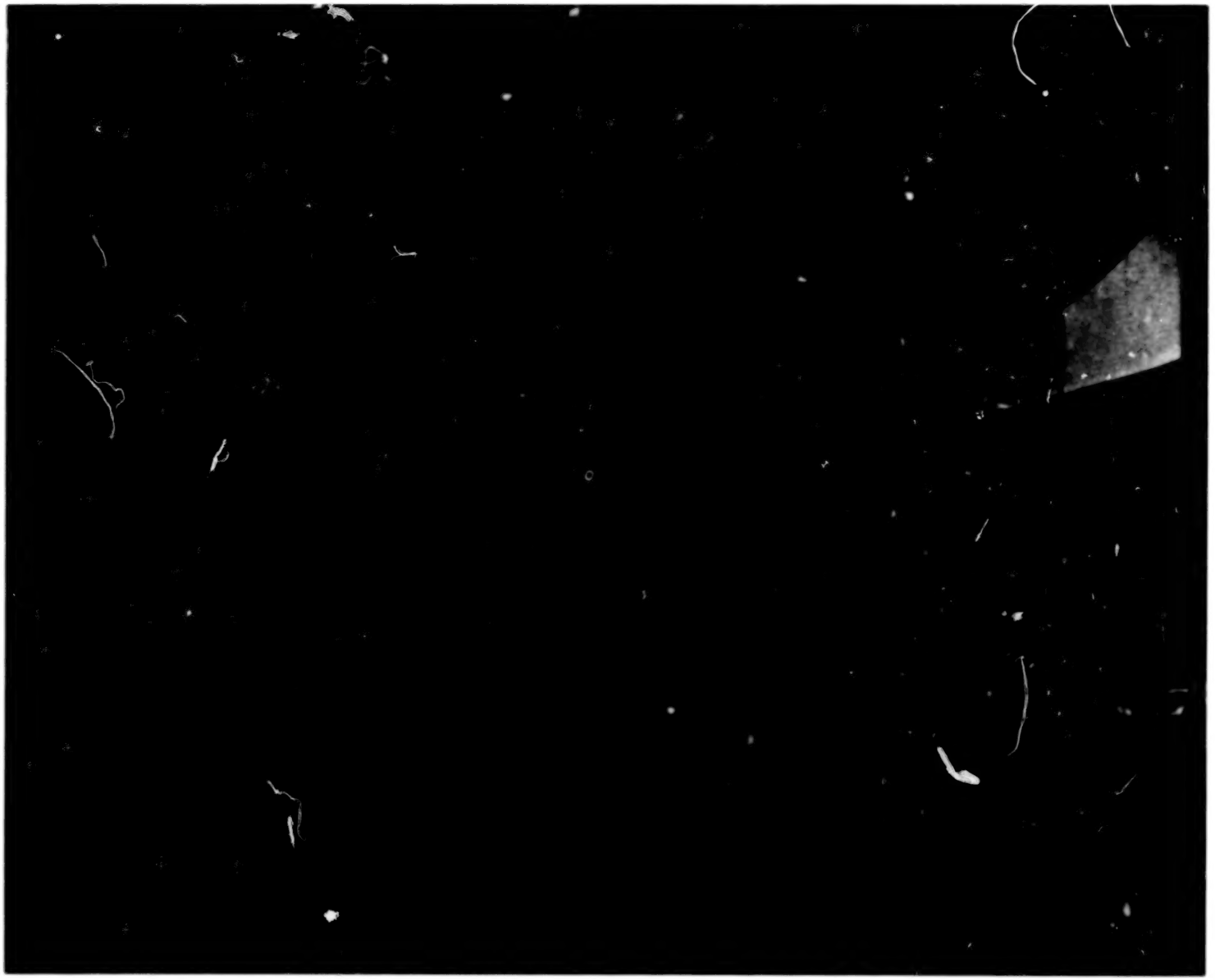

L-77-249

Figure 14.- Typical flow field in the fluidic amplifier with a deflected jet resulting from a differential input pressure.

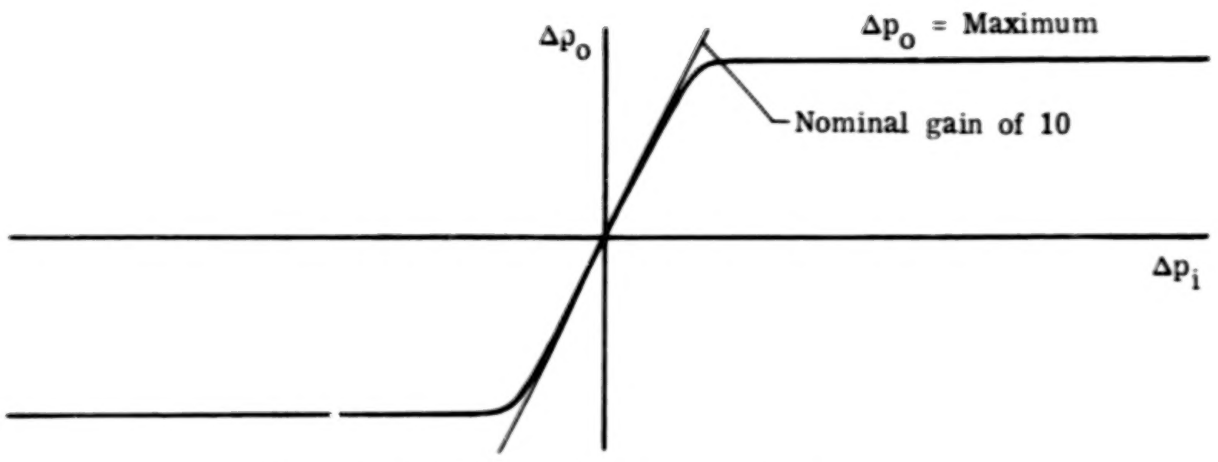

(a) Flat maximum differential output pressure.

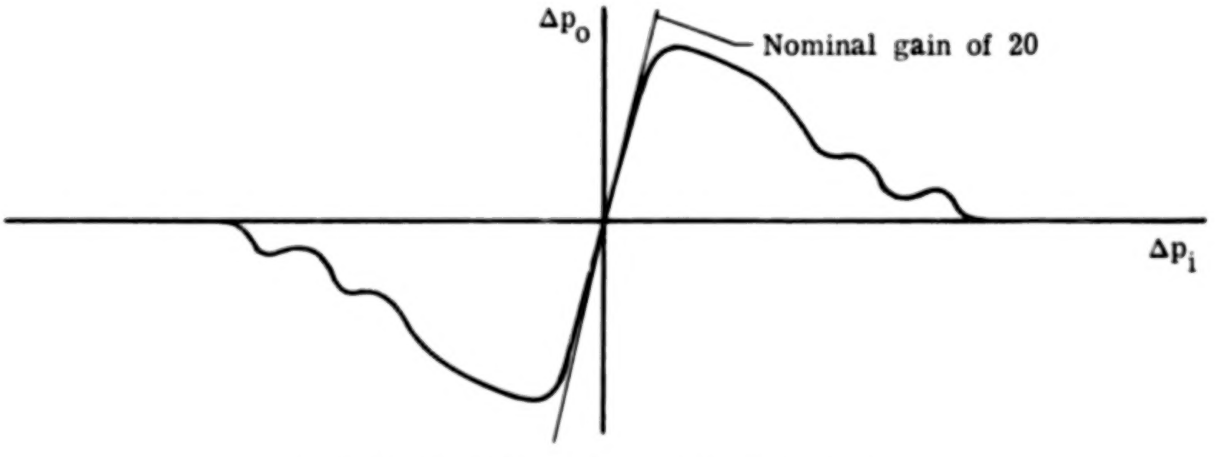

(b) Reduced differential output pressure.

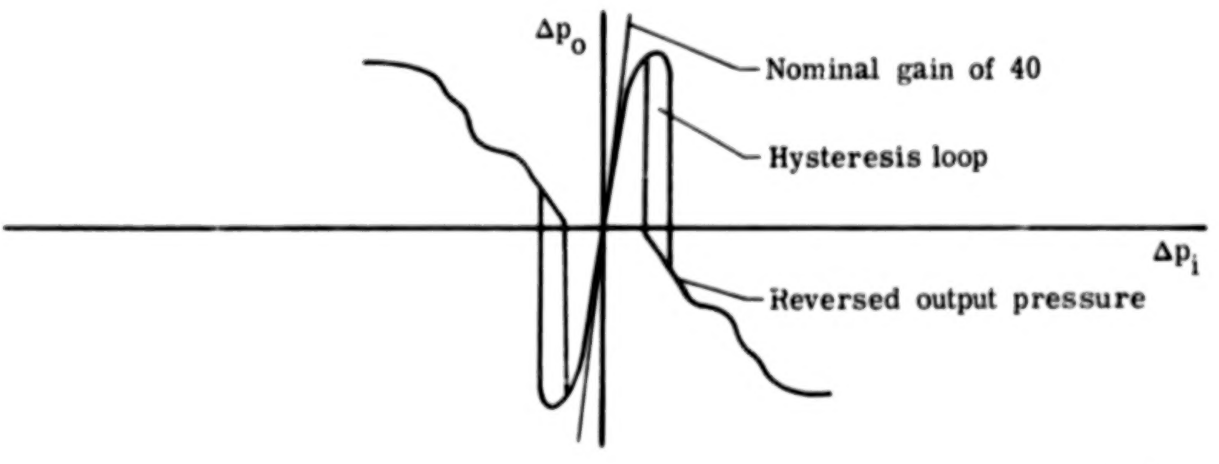

(c) Reversed differential output pressure.

Figure 15.- Conceptual pressure gain for three saturation characteristics.

L-77-250

Figure 16.- Supply stream deflected off downstream edge of input duct.

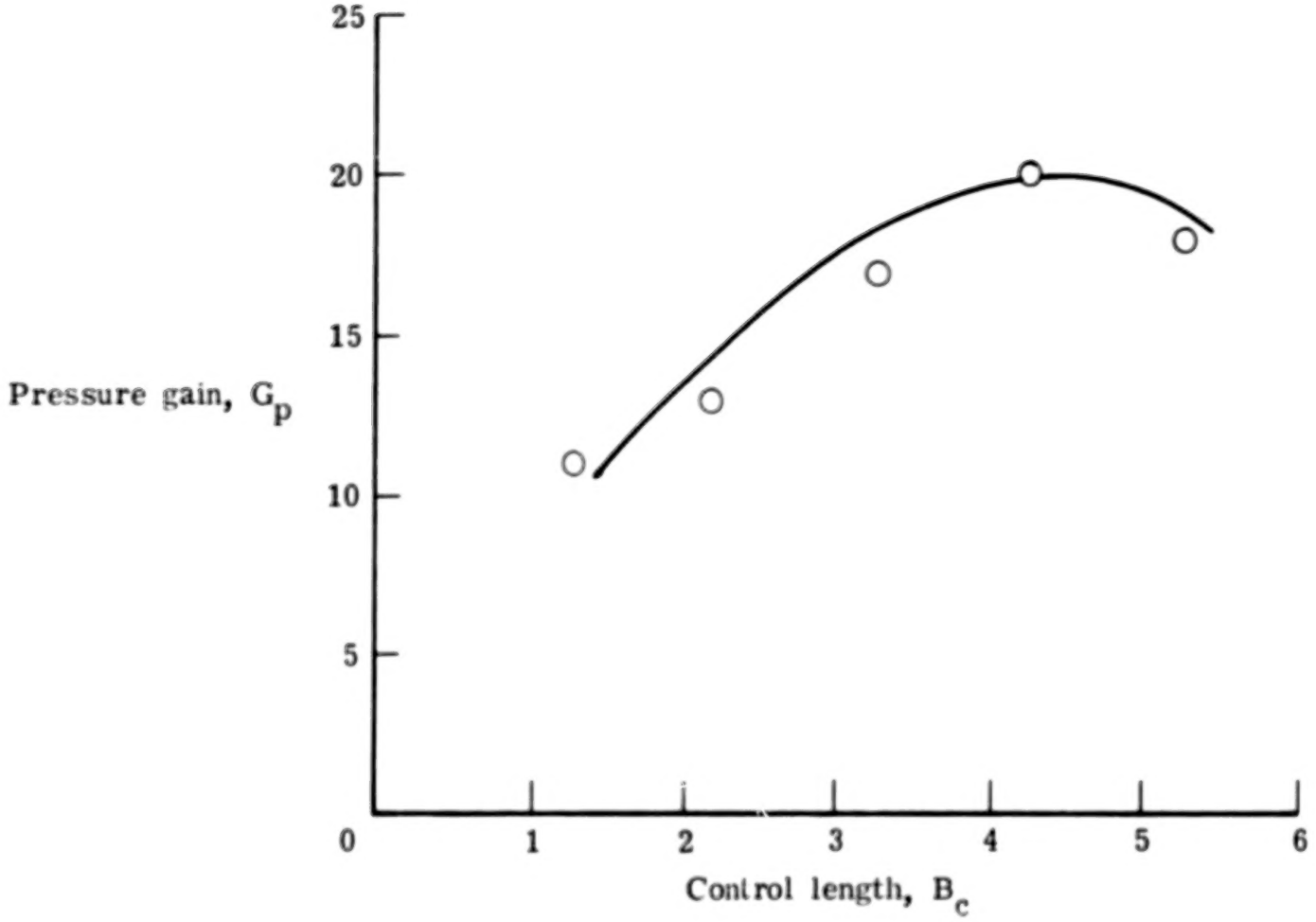

Figure 17.- Pressure gain as a function of control length.

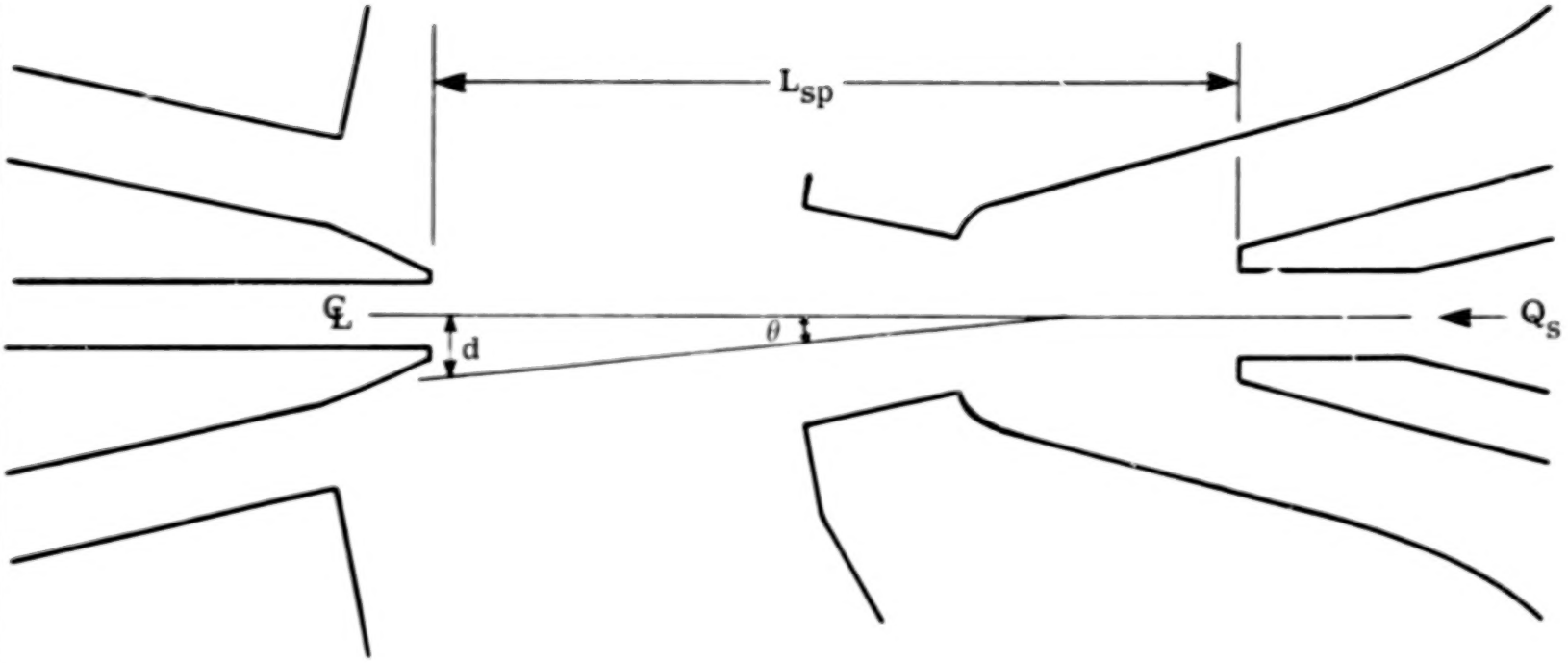

Figure 18.- Center line of supply jet stream deflected through angle θ. $d = L_{sp} \tan \theta$.

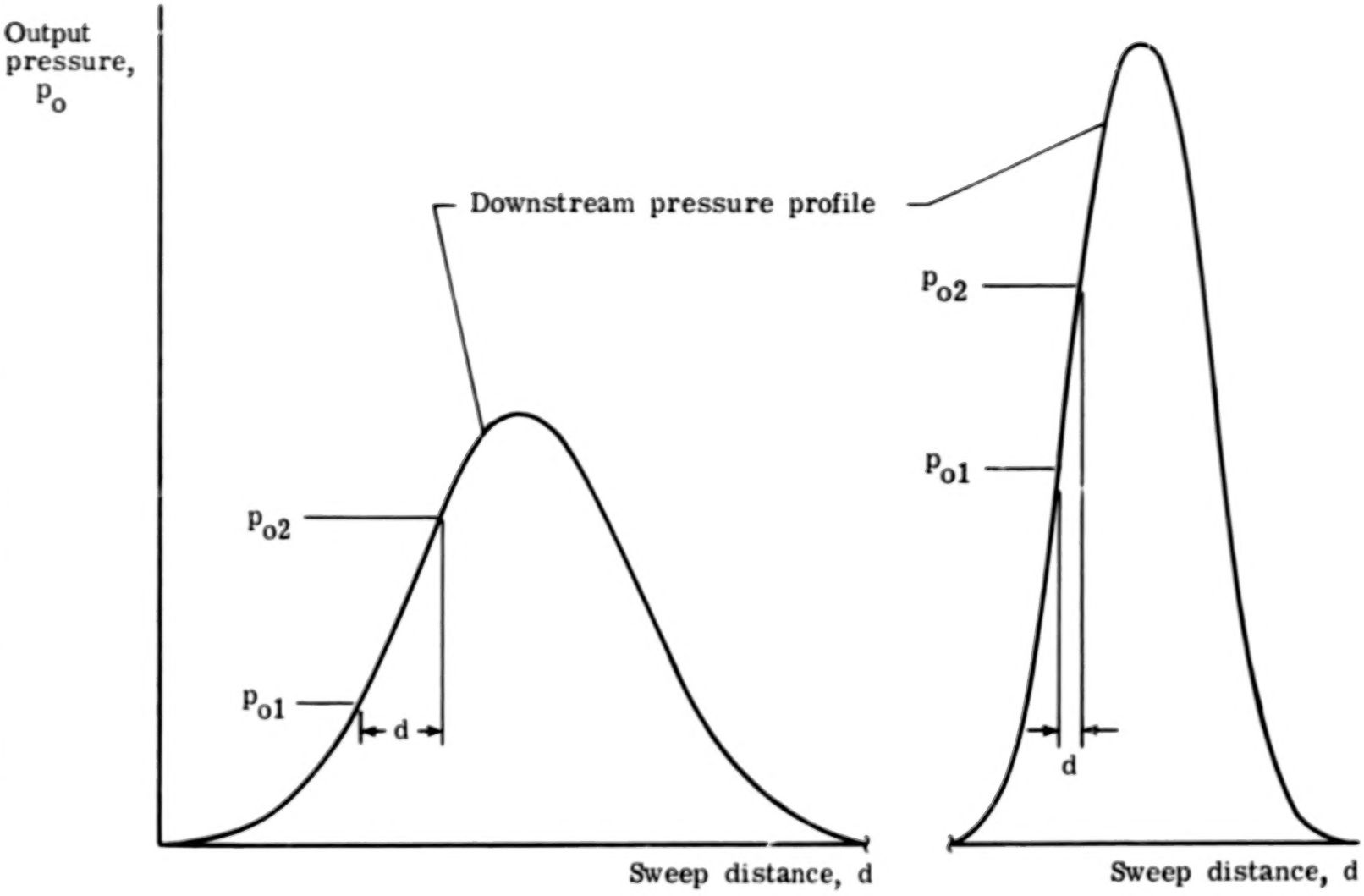

(a) Long splitter distance.

(b) Short splitter distance.

Figure 19.- Conceptual output-pressure profiles as function of sweep distance for two amplifiers of different splitter distances.

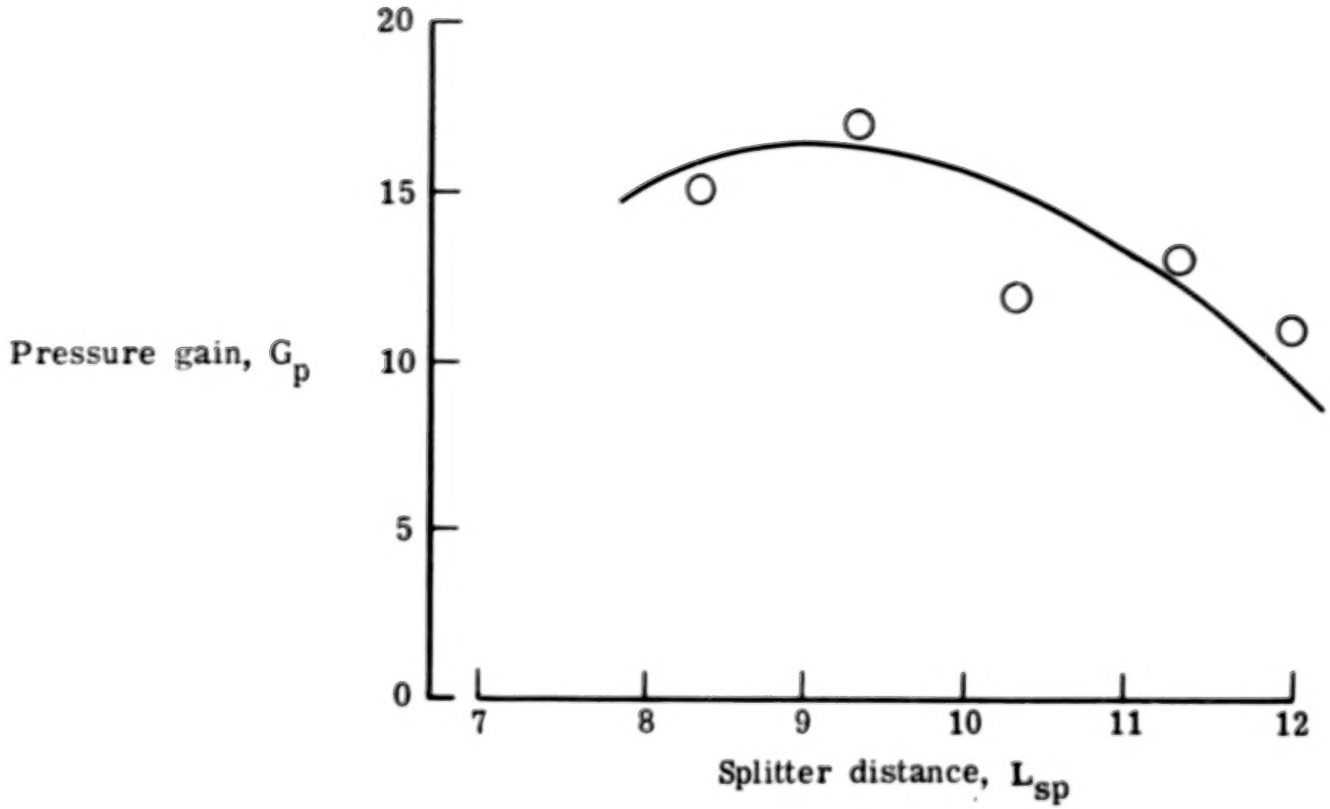

Figure 20.- Pressure gain as function of splitter distance.

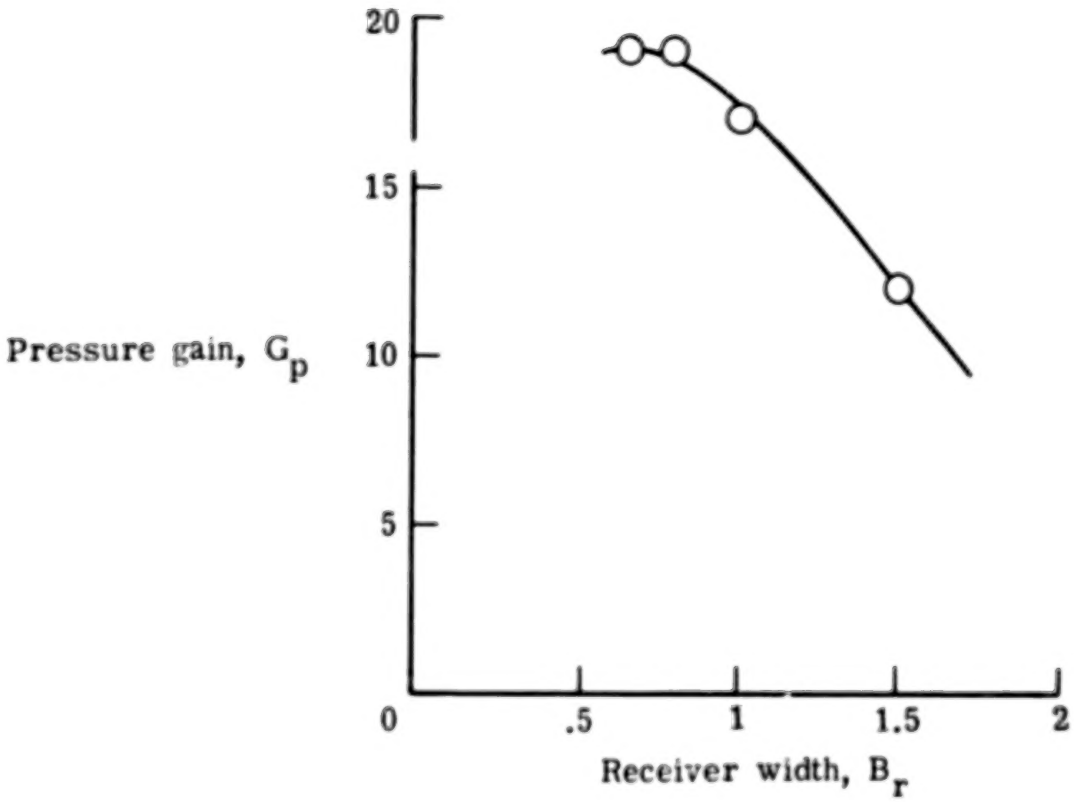

Figure 21.- Pressure gain as function of receiver width.

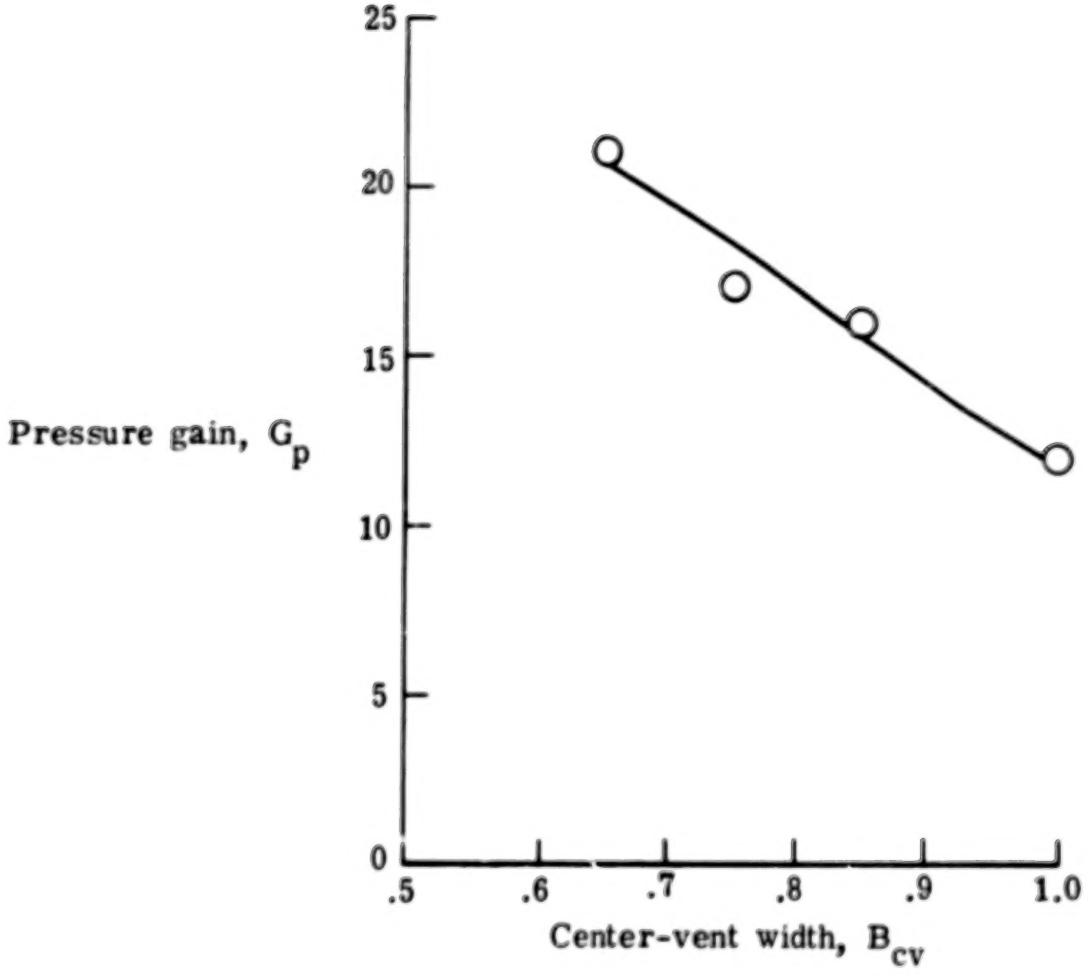

Figure 22.- Pressure gain as function of center-vent width.

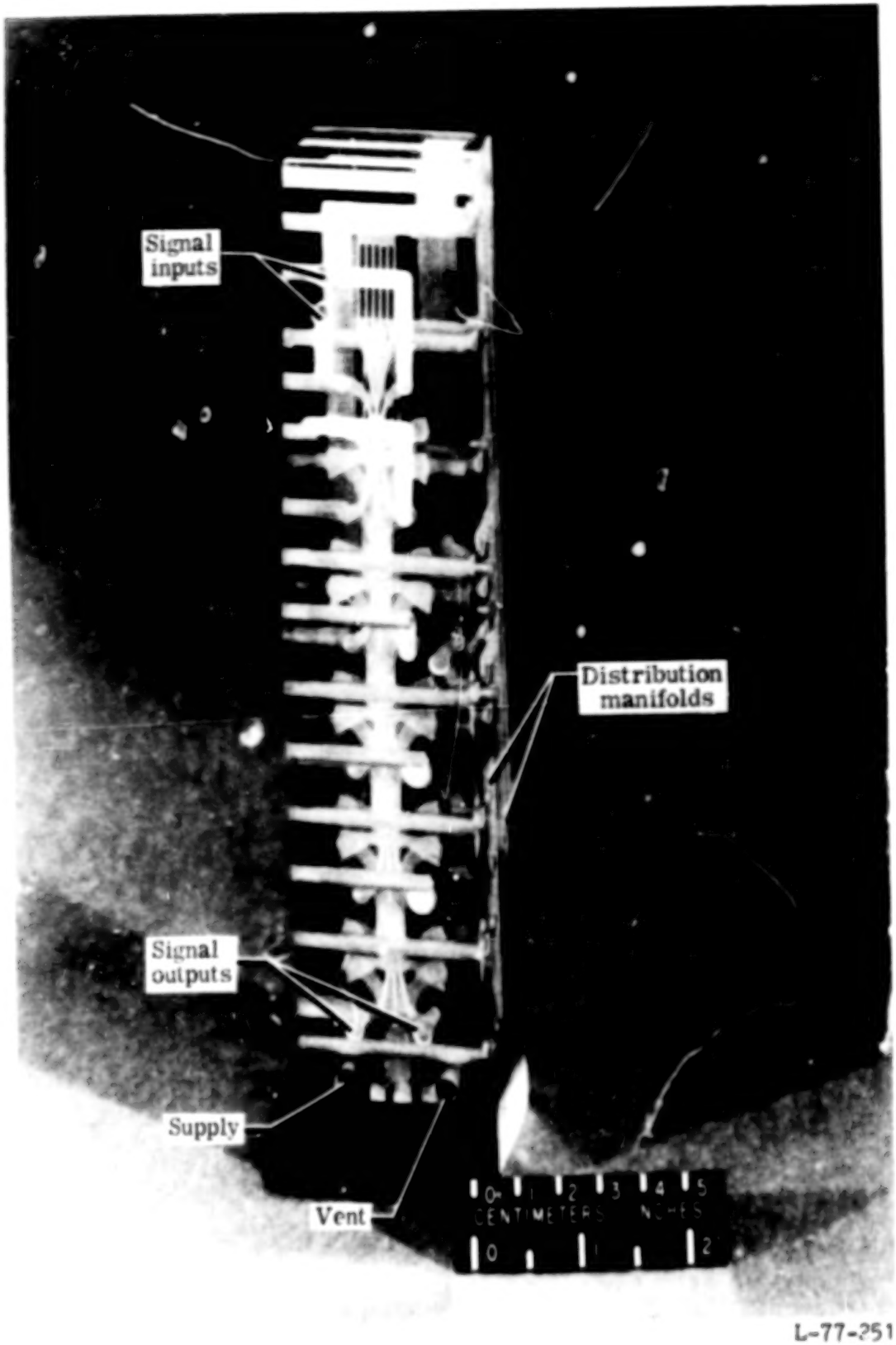

L-77-251

Figure 23.- Five amplifiers internally connected with supply and vent manifolds G_p = 100 000.

A motion-picture film supplement L-1228 is available on loan. Requests will be filled in the order received. You will be notified of the approximate date scheduled.

The film (16 mm, 20 min, color, sound) shows flow-visualization studies of the laminar flow in a proportional fluidic amplifier under varying operating conditions.

Requests for the film should be addressed to:

NASA Langley Research Center
Att: Photographic Branch, Mail Stop 425
Hampton, VA 23665

CUT

Date _____

Please send, on loan, copy of film supplement L-1228 to NASA TN D-8433.

_____
Name of organization

_____
Street number

_____
City and State Zip code

Attention: Mr. _____

Title _____

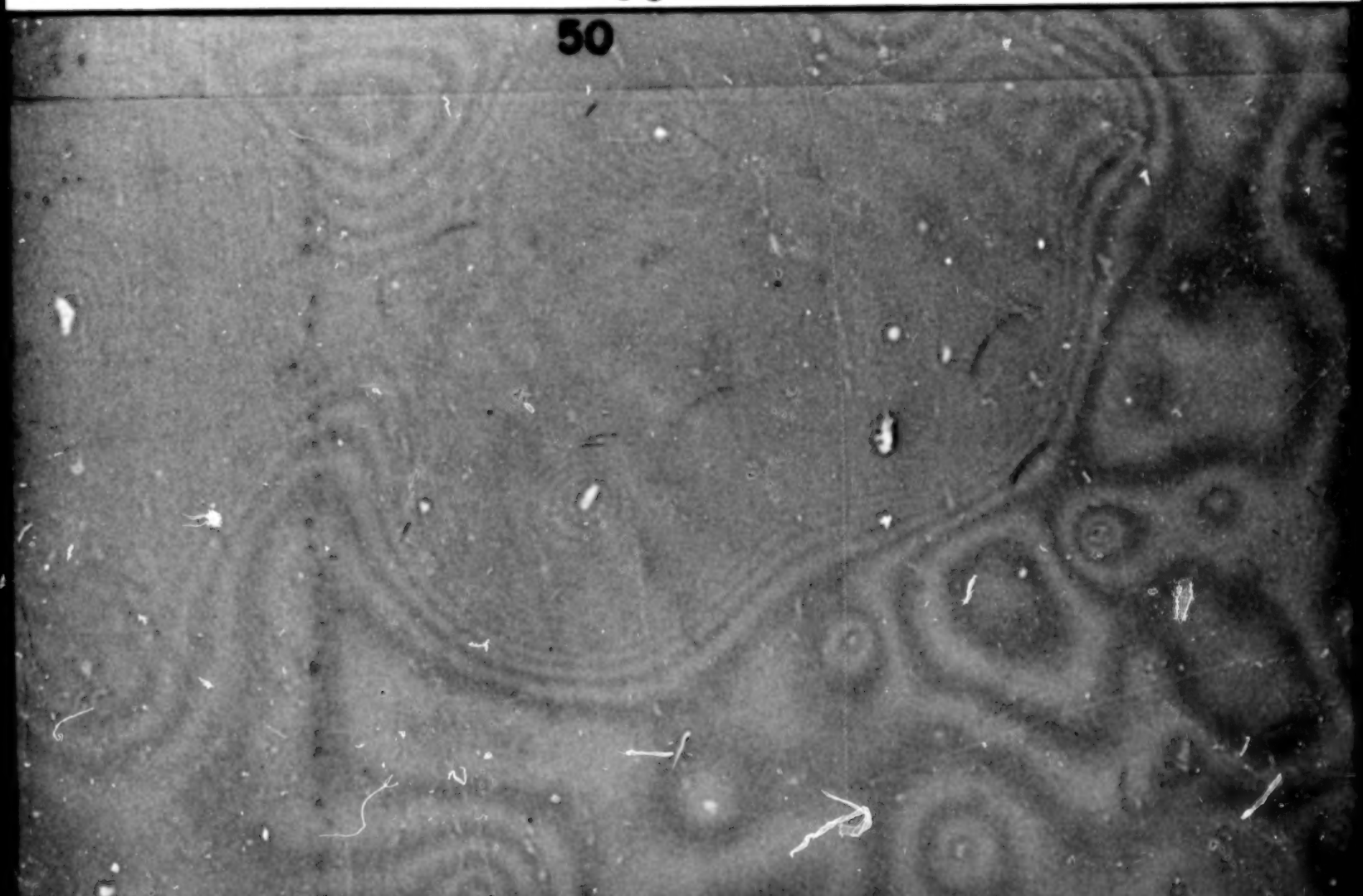
90
50

END

5.19 78